

# D10.1

## Method for rapid seismic loss estimation

# D10.1 Method for rapid seismic loss estimation

Dissemination Level: Public  
 Lead Partner: INFP  
 Due date: December 2024  
 Actual submission date: 27 December 2024

**PUBLISHED IN THE FRAMEWORK OF**  
 MULTICARE (Horizon Europe grant 101123467)

## AUTHORS

INFP: Toma-Danila Dragos, Tigianescu Alexandru, Marmureanu Alexandru, Grecu Bogdan, Cioflan Carmen Ortanza, Neagoe Cristian, Coman Alina

## REVISION AND HISTORY CHART

VERSION	DATE	EDITORS	COMMENT
<b>V0.1</b>	26 NOV 2024	Toma-Danila Dragos, Tigianescu Alexandru, Grecu Bogdan (INFP)	Draft
<b>V0.2</b>	3 DEC 2024	Coman Alina, Cioflan Carmen Ortanza (INFP)	Draft
<b>V0.3</b>	6 DEC 2024	Toma-Danila Dragos, Tigianescu Alexandru, Grecu Bogdan, Marmureanu Alexandru, Neagoe Cristian (INFP)	Draft
<b>V0.4</b>	20 DEC 2024	Pedone Livio (Sapienza University of Roma)	Review
<b>V1.0</b>	23 DEC 2024	Toma-Danila Dragos, Tigianescu Alexandru (INFP)	Final Version

## DISCLAIMER

The information in this document is subject to change without notice. Company or product names mentioned in this document may be trademarks or registered trademarks of their respective companies.

### **All rights reserved**

The document is proprietary of the MULTICARE consortium members. No copying or distributing, in any form or by any means, is allowed without the prior written agreement of the owner of the property rights.

This document reflects only the authors' view. The European Community is not liable for any use that may be made of the information contained herein. Responsibility for the information and views expressed in the therein lies entirely with the author(s).

# Table of contents

1. Introduction.....	8
2. Overview of RSLE methodologies.....	9
2.1. Seismic hazard estimation.....	10
2.2. ShakeMap methodology.....	17
ShakeMap v3.5.....	19
ShakeMap v4.0.....	23
2.3. Damage and loss estimation methods.....	27
Fragility functions.....	28
Consequence functions.....	31
Vulnerability functions.....	32
Databases for fragility and vulnerability functions.....	34
Structural typologies and exposure modelling.....	34
2.4. Triggered hazard analysis.....	35
2.5. Overview of RSLE software available.....	37
3. Concept for the Multicare RSLE.....	55
Envisioned methodology.....	55
Preliminary testing.....	57
3. Conclusion.....	63
Annex 1. List of countries that have implemented ShakeMap.....	64
References.....	66

## LIST OF FIGURES:

Figure 1. Four basic steps of PSHA (Reiter, 1991).....	11
Figure 2. Seismic hazard curves (mean values) of ESHM20 model (Danciu et al., 2021) for several highly populated cities in Romania.....	13
Figure 3 Hazard curves example: full distribution of hazard curves for 10 000 samples of the ESHM20 main logic tree. Mean and five quantiles (5th, 16th, 50th, 84th, 95th) are given for Bucharest (Romania), Istanbul (Türkiye), Zagreb (Croatia), Syracuse (Italy), Lisbon (Portugal), and Stockholm (Sweden). These results are applicable to generic rock soil conditions with a shear wave velocity ( $V_{s30}$ ) of $800 \text{ ms}^{-1}$ (from Danciu et al., 2024).....	13
Figure 4. NHVSR and EHVS curves for the stations located far-field (left) and close-field (right) related to earthquakes in the Gorj, Romania 2023 sequence (colored lines).....	16
Figure 5. Response spectra for the analyzed seismic events (the colored lines are unitary as in Figure 4) for far-field (left) and close-field (right), related to earthquakes in the Gorj, Romania 2023 sequence. ....	16

Figure 6 Schematic main principles of the ShakeMap workflow (after Guerin-Marthe et al., 2021).....	23
Figure 7. Fragility curves for masonry (thin lines) and reinforced concrete (thick lines) building typologies converted to PGA (left) and Sa(0.3s) (right) (Michel et al., 2018).....	29
Figure 8. Main components and phases considered in analytical fragility assessment methodologies and associated uncertainties (Maio & Tsionis, 2015).....	31
Figure 9 Fatality rates (a) and estimated number of casualties (b) as a function of damage level and building type related to the DB L'Aquila urban area for two models: NRA and Z&C (from Manfredi et al., 2023).....	32
Figure 10 Example of earthquake vulnerability functions for Central Asian residential buildings and infrastructure assets (from Salgado-Gálvez et al., 2024).....	32
Figure 11 Cumulative distribution function of (a) repair cost and (b) repair time (from You et al., 2023).....	33
Figure 12 left) Comparison between the OR function as proposed by Coburn and Spence (2002) (for urban population, dotted blue line, and rural population, dashed blue line) and that proposed by the authors of the present paper; right) Occupancy rate function for weekdays (dashed blue line, only weighted over the municipality size) and holidays (dashed red line, only weighted over the municipality size). The solid black line refers to function weighted over the number of weekdays and holidays in one year. (from Manfredi et al., 2023).....	33
Figure 13. Screenshots of interactive map for the Loma Prieta earthquake for landslide hazard (left) and liquefaction hazard (right). Insets show zoom-in on the area indicated. (source: USGS, 2024a).....	36
Figure 14 Flowchart of SISMOTOOL (Lopez Hidalgo et al., 2022).....	52
Figure 15 SISMOTOOL development and computation scheme (Lopez Hidalgo et al., 2022).....	53
Figure 16 SELENA computational flowchart (from Molina et al., 2010).....	54
Figure 17 OpenQuake Scenario Damage (left) and Risk (right) Calculator input/output structure (GEM, 2024).....	54
Figure 18 Proposed framework for the MULTICARE RSLE system.....	57
Figure 19 Ground motion distribution map (in PGA), for a scenario of the March 4, 1977 Vrancea earthquake (Mw 7.7, 94 km depth), using 3 ground motion prediction equations (GMPE): a) and b) Sokolov et al. (2008), c) and d) Vacareanu et al. (2015), e) and f) Manea et al. (2022), and untruncated and truncated forms with coefficient 1 of the equations.....	58
Figure 20 Ground motion distribution map (in PGA values), for a crustal earthquake scenario in the Tecuci area (Mw 6.0, 20 km depth), obtained for the untruncated form of 4 GMPEs: a) Boore et al. (2014), b) Cauzzi et al. (2014), c) Chiou and Youngs (2014) and d) Kale et al. (2015; Iran).....	59
Figure 21 Ground motion distribution map (in PGA values), for a crustal earthquake scenario in the Tecuci area (Mw 6.0, 20 km depth), obtained for the truncated 1 form of 4 GMPEs: a) Boore et al. (2014), b) Cauzzi et al. (2014), c) Chiou and Youngs (2014) and d) Kale et al. (2015; Iran).....	60
Figure 22 Estimates of the number of completely damaged residential buildings, obtained for scenarios of the March 4, 1977 Vrancea earthquake (Mw 7.7, 94 km depth; with truncation levels 0 and 1); the minimum (top), median (middle) and maximum (bottom) values are shown, obtained with the ESRM20 fragility function set for ShakeMap (a, c and e) and Various (b, d and f).....	61
Figure 23 Estimates of the number of completely damaged residential buildings, obtained for crustal earthquake scenarios in the Tecuci area (Mw 6.0, 20 km depth; with truncation levels 0 and 1); the minimum (top), median (middle) and maximum (bottom) values are shown, obtained with the ESRM20 fragility function set for ShakeMap (a, c and e) and Various (b, d and f).....	62
Figure 24 Estimates of the number of persons severely injured or deceased, obtained for a scenario of the earthquake of March 4, 1977 (Mw 7.7, 94 km depth); the minimum (top),	

median (middle) and maximum (bottom) values are presented, obtained with the set of vulnerability functions from ESRM20 for ShakeMap (a, c and e) and Various (b, d and f).... 63

## LIST OF TABLES:

Table 1. Summary of Key Earthquake-Triggered Hazards.....	35
Table 2. Comparison of software capable of RSLE implementation (in alphabetical order) .....	37

## GLOSSARY

ACRONYM	FULL NAME
CA	Consortium Agreement
EC	European Commission
EASME	The Executive Agency for Small and Medium-sized Enterprises
GA	Grant Agreement
PC	Project Coordinator
WP	Work Package
TL	Task Leader
DoA	Description of Action
PSC	Project Steering Committee
SQM	Scientific and Quality Manager
DEC	Dissemination and Exploitation Committee
KOM	Kick-off meeting
GER	General Exploitable Result
AB	Advisory Board
PM	Person month
M	Month
INFP	National Institute for Earth Physics, Romania
TUD	Delft University of Technology, Netherlands
RSLE	Rapid Seismic Loss Estimation

# 1. Introduction

Rapid seismic loss estimation is highly important in the context of minimizing the impact of an earthquake and aiding in recovery efforts. Here are some key points explaining its significance:

1. **Timely Response and Resource Allocation:** After an earthquake, there is an urgent need for emergency response teams to assess the damage quickly. Rapid seismic loss estimation helps authorities and agencies prioritize where to send resources, medical aid, rescue teams, and other critical support. This can save lives and reduce further destruction.
2. **Public Safety:** Immediate damage assessments can inform decisions about evacuations, road closures, and other safety measures. If the extent of structural damage to buildings, bridges, and infrastructure is known quickly, it helps prevent injuries or fatalities caused by unsafe structures.
3. **Insurance and Financial Implications:** Accurate loss estimation assists insurance companies, governments, and businesses in assessing the economic impact of an earthquake. It provides a foundation for quick financial claims processing, compensation distribution, and identifying areas that need economic recovery support.
4. **Infrastructure Recovery:** Earthquakes can severely disrupt transportation, communication, water, power, and other critical infrastructure. Rapid seismic loss estimation identifies the most affected areas, enabling swift planning for repair and restoration of services.
5. **Planning and Risk Mitigation:** Rapid loss estimation contributes to understanding seismic risk in a region and potential multi-hazard and multi-risk implications. This knowledge allows for more effective planning for future events, including retrofitting buildings, improving building codes, and reinforcing infrastructure to reduce future losses.
6. **Political and Public Confidence:** Governments and local authorities need to demonstrate to the public and other stakeholders that they can respond effectively to a disaster. Rapid and reliable damage assessment helps reassure citizens and fosters trust in leadership during a crisis.
7. **Humanitarian Aid and Relief Coordination:** International aid organizations, NGOs, and local agencies rely on seismic loss estimates to coordinate relief efforts. A timely estimate ensures that aid reaches the right locations and supports the populations most affected.

Given that loss estimation relies on hazard models with still significant limitations and validation, as well as ever-changing socio-economic exposure and vulnerability datasets, it is to be seen as a dynamic and continuous process. Quantification of uncertainties (both epistemic and aleatory) is crucial to highlight the limits of seismic loss estimations. Results, whether in terms of affected buildings, people, or economic losses, have a high degree of sensitivity which needs to be understood, therefore it is not always suitable to pass them to uninformed stakeholders or the public.

**In this deliverable we will present some of the main methods for rapid seismic loss estimation (RSLE), with a focus on determining their potential, limitations, and contribution to achieving the MULTICARE Project objectives.** MULTICARE envisions the development of an RSLE system with the following requirements:

- Provide rapid estimation of building seismic damage and socio-economic losses in the Tecuci and Bucharest case-study areas (but flexible enough to be implemented elsewhere);

- Exploit Earthquake Early Warning capabilities in earthquake detection and rapid communication (before communication breakdowns intervene) and crowd-sourced data from sources such as “Did you feel it?” data;
- Provide options to improve exposure and vulnerability models by using:
  - o remote sensing data and deep learning algorithms for building classification;
  - o monitoring data from typologically representative buildings with accelerometer sensors installed;
  - o post-earthquake inspection data;
  - o vulnerability factors reflecting time degradation (due to climate change, major earthquakes, flooding etc.).
- Be capable of including or linking to multi-hazard analysis modules, in the context of possible earthquake-triggered events (e.g. liquefaction, landslides, tsunamis or floods).

## 2. Overview of RSLE methodologies

Over the time, multiple methodologies devoted to the estimation of structural damage, human and economic losses due to earthquakes have been developed. The demand for such methodologies is both scientific but also practical, with results being of high interest in emergency management, risk reduction strategies or the insurance sector. In its sense, macroseismic intensity – a subjective descriptor of earthquake effects, was used in evaluating the potential effects of earthquakes long before magnitude calculation. Initially, simple methods for estimating what could the losses be after an earthquake were developed using equations built upon correlations of intensity with damage observations. As new equipment and technologies became available, as well as real data from seismic events, more attention was drawn to the understanding of earthquake effects on buildings (as “not earthquakes kill people so much, but building behavior”) and linking damage degrees with the probability of injury or economic losses. Coupled with progress in seismic instrumentation equipment, building information modeling or experimental testing increased capacities, progress was significantly made in understanding building behavior during various types of earthquakes and methods for representing potential damage as a function of intensity measures were developed - fragility functions. To make a link between structural damage and socio-economic loss, consequence functions were developed. Vulnerability functions – capable of directly reflecting losses for a specific building typology, were also elaborated, as a more direct approach from ground motion intensity measures to direct losses. Indirect impact was also expressed, using vulnerability but also resilience functions. Nowadays there are multiple methodologies and software for estimating rapidly after an earthquake damage and loss levels, but there are still significant challenges:

- how to better account for local site effects?
- how to account for time dependencies in seismic hazard (e.g., mainshock-aftershock sequences, triggered seismic events), multi-hazard and multi-risk scenarios?
- how to describe more accurately, using fragility functions or other methods, the variability in the distribution of structures in different areas but also variability within the building typology?
- how to quantify and express uncertainty?
- how to consider structure degradation, seismic damage accumulation, habitability, and economical evolution effects throughout the time in vulnerability models?
- how to quickly integrate real observation in new or altered vulnerability models?

## 2.1. Seismic hazard estimation

Seismic hazard analyses can be performed using two general approaches: deterministic seismic hazard analysis (DSHA) and probabilistic seismic hazard analysis (PSHA). Each of them has advantages for various purposes but also limitations. DSHA focuses on the worst-case scenario (or a specific earthquake scenario) and provides deterministic results, while PSHA integrates probabilistic information and uncertainties to give a more comprehensive risk assessment. PSHA is more widely used for long-term seismic hazard mapping and risk management, while DSHA is often used for immediate design purposes or regulatory assessments based on the maximum ground shaking expected. With regards to an RSLE system, a DSHA-like approach (scenario-based) is more suitable, but providing also means for PSHA can be beneficial for planning purposes.

**The deterministic seismic hazard analysis (DSHA)** is used when the consequences of failure are intolerable and suitable protection is required. Then, the worst event that can be reasonably expected to occur at the site is usually evaluated. This event can be regarded, for example, as the maximum credible earthquake (MCE) maximizing the effects at the spectral frequencies for which the critical facility & infrastructure is more sensitive for its structural safety and serviceability.

DSHA is an approach in which the hazard is estimated as maximum ground motion based on parameters of a single earthquake or set of earthquakes. To perform DSHA three basic elements have to be specified (Reiter, 1991): earthquake source, controlling earthquake of the particular size and level of seismic ground motion characteristic at selected distance. Consequently, seismic hazard can be expressed as a resulting value of specified ground motion characteristics following the occurrence of causative earthquake originating from a particular source at a specified distance. DSHA is comprised of four basic steps:

1. *The identification of seismic source zones.* Individual sources may have the character of points, lines, areas or volumes. In order to identify these sources, the seismological, geological, geotechnical and geophysical databases are compiled. The content of these databases can vary based on the purpose of the analysis.
2. *The selection of the controlling earthquake.* Maximum earthquake in terms of magnitude is assigned to each source zone. Also, the closest distance of each source zone from the site of -interest is determined. Controlling earthquakes is the one whose characteristics at the site of interest are dominant in comparison with characteristics of the maximum earthquakes from other source zones. Selection of the controlling earthquake may be a difficult task (Baker, 2008). If faults in the vicinity of the site are poorly mapped, the seismic source zone is defined as an area and earthquakes can occur in any part of this zone. If the site is found to be exactly in the seismic source zone, it is assumed that the location of the maximum earthquake is right under the study site.
3. *The selection of the appropriate ground motion model (GMM, formerly known as ground motion prediction equations - GMPE).* GMMs, previously known as attenuation relationships, estimate the value of chosen ground motion characteristics for an earthquake characterized by source parameters, distance and site conditions (Douglas and Gkimprixis, 2018).
4. *The estimation of the seismic hazard at the site of interest.* Basically, it is the combination of the steps mentioned above and the estimation of the ground motion characteristic according to the magnitude and distance of the causative earthquake using GMM.

**The Probabilistic seismic hazard analysis (PSHA)** allows estimation of the probability that selected ground motion parameters will be exceeded, at a given site, within a certain time interval (Cornell, 1968). It represents a powerful tool that integrates all earthquake occurrences, in space and time, surrounding a selected study site. Unfortunately, the concept of a causative earthquake is lost when performing a PSHA. That is, there is no specific earthquake, in terms of magnitude and source-to-site distance, reproducing the uniform hazard spectrum (UHS) at the selected exceedance probability within a reference time return period.

Unlike DSHA, probabilistic seismic hazard analysis is not constrained to maximum earthquake but rather comprises effects of all earthquakes of all magnitudes up to a predefined source-to-site distance, which can affect ground motion at the site of interest (Kramer, 1996; Baker, 2008). PSHA allows the inclusion of various alternatives of input data into computation, along with their associated uncertainties. Seismic hazard can be expressed as the annual probability of exceeding a selected level of ground motion characteristic. The results of the analysis can be used to estimate seismic risk.

Four basic steps of the PSHA are illustrated in Figure 1. The prerequisite of this computation is the compilation of the aforementioned databases for the site of interest, similarly as for DSHA. The content of the databases can vary, due to the purpose of the analysis. The data should comprise the following information about the earthquakes: coordinates of the epicenter, depth of the focus, all determined magnitudes and seismic moment, maximum and epicentral intensity along with the type of the scale, description of the observed damage, isoseismal map, estimation of the uncertainty for each of the parameters mentioned, information about felt foreshocks and aftershocks. Beneficial is also knowledge on focal mechanism.

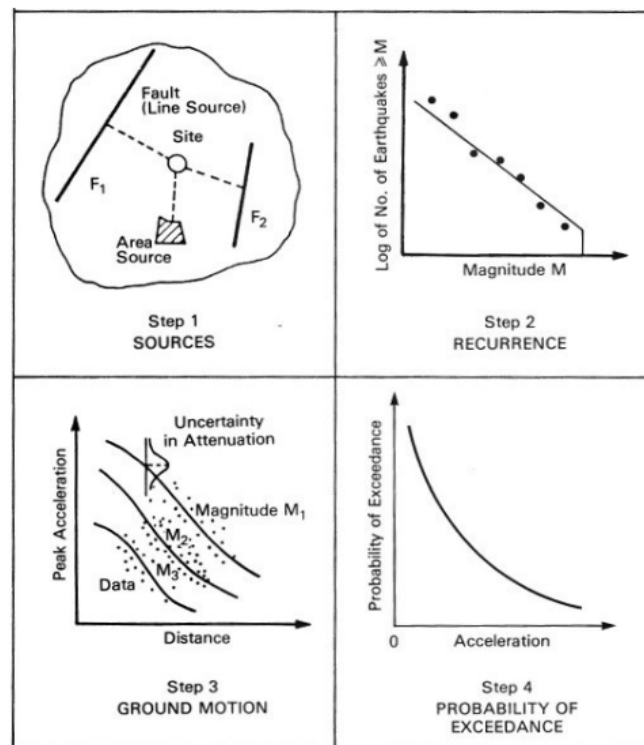


Figure 1. Four basic steps of PSHA (Reiter, 1991)

Steps in PSHA:

1. *The identification of seismic source zones.* In this step the PSHA is analogous to DSHA, individual sources may have character of points, lines, areas or volumes. Seismotectonic model is composed of the synthesis of seismological, geological, geotechnical and geophysical databases. Consequently, two types of seismic sources can be distinguished. Seismogenic structures are defined from the data of geological and seismological databases based on the features for which exists direct or indirect evidence that were active in the last tectonic regime. Diffuse seismicity zones are those where no apparent correlation can be made between earthquakes with any specific geological structures.
2. *The determination of the recurrence law and maximum magnitude, together with associated uncertainties, for each source zone.* Recurrence law is the relation between the magnitude of the event with its occurrence frequency inside the source zone during a selected time window T (usually considered annually). This step is significantly different from the DSHA. Prior to the computation of the parameters in recurrence law, it is inevitable to process the seismological database. A consistent type of magnitude, usually  $M_w$ , for each earthquake has to be determined (homogenization), and foreshocks, mainshocks and aftershocks have to be separated (catalogue declustering). Estimation of the temporal and spatial completeness of the database in terms of magnitude must be performed. Most frequently the Gutenberg and Richter (1944) recurrence law is used in the form:

$$\log_{10} N(m) = a - bm \quad (1)$$

where  $N(m)$  is the annual rate of exceedance of magnitude  $m$  and  $m \geq 0$  (Reiter, 1991). Constant  $a$  is the mean yearly number of earthquakes with magnitude larger or equal to zero and the constant  $b$  determines the ratio of strong to weak earthquakes in each seismic source.

3. *The determination of earthquake effects.* Since in PSHA earthquakes of all magnitudes and from all distances in seismic source zones are included in the computation, equations related to selected ground motion characteristics must be considered along with the estimated uncertainties. The effects are estimated using empirical GMMs for selected ground motion characteristics. GMMs are usually functions of magnitude, source-to-site distance and other relevant parameters (e.g. local conditions, style of faulting) (Douglas, 2018). These models also comprise random error terms, assumed as normally distributed with zero mean and standard deviation  $\sigma$ . This term represents the aleatory uncertainty of ground motion.
4. *The estimation of the seismic hazard at the study site.* This step is significantly different compared to DSHA. In PSHA effects of all earthquakes of all magnitudes and distances along with uncertainties, contribute to hazard output. The result of PSHA is a seismic hazard curve which can be expressed as the annual probability of exceedance of a specified level of ground motion intensity at the site of interest (Figure 2). Alternatively, the curve can be expressed as annual frequency (or mean return period) in which a specified level of ground motion characteristic will be exceeded at the site. The results are not determined as single values but as a probability distribution function. Therefore, usually median, 84 percentile and mean hazard curves are estimated (Figure 3). The 84 percentile is presented as mean plus one standard deviation. The one-standard-deviation bounds should enclose about

2/3 of the observed values if the uncertainties are normally distributed. A thorough explanation of the methodology of computing percentiles can be found in background documents of the relevant software CRISIS 2007 (Ordaz et al., 2007).

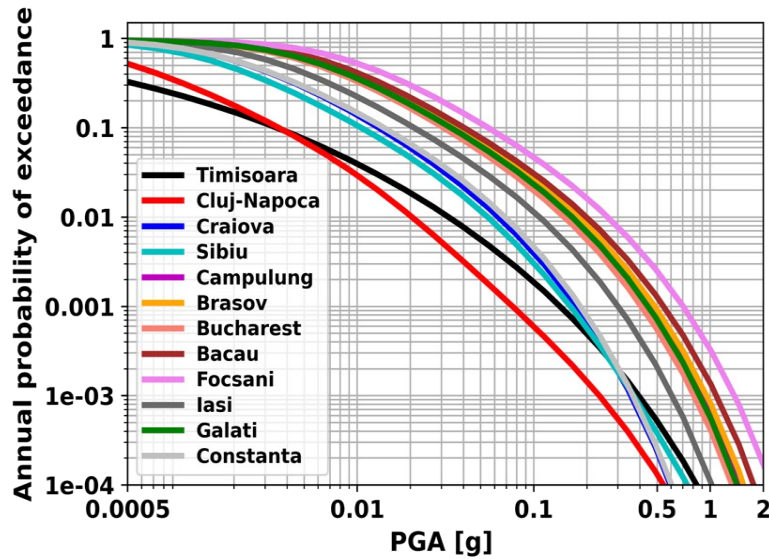


Figure 2. Seismic hazard curves (mean values) of ESHM20 model (Danciu et al., 2021) for several highly populated cities in Romania.

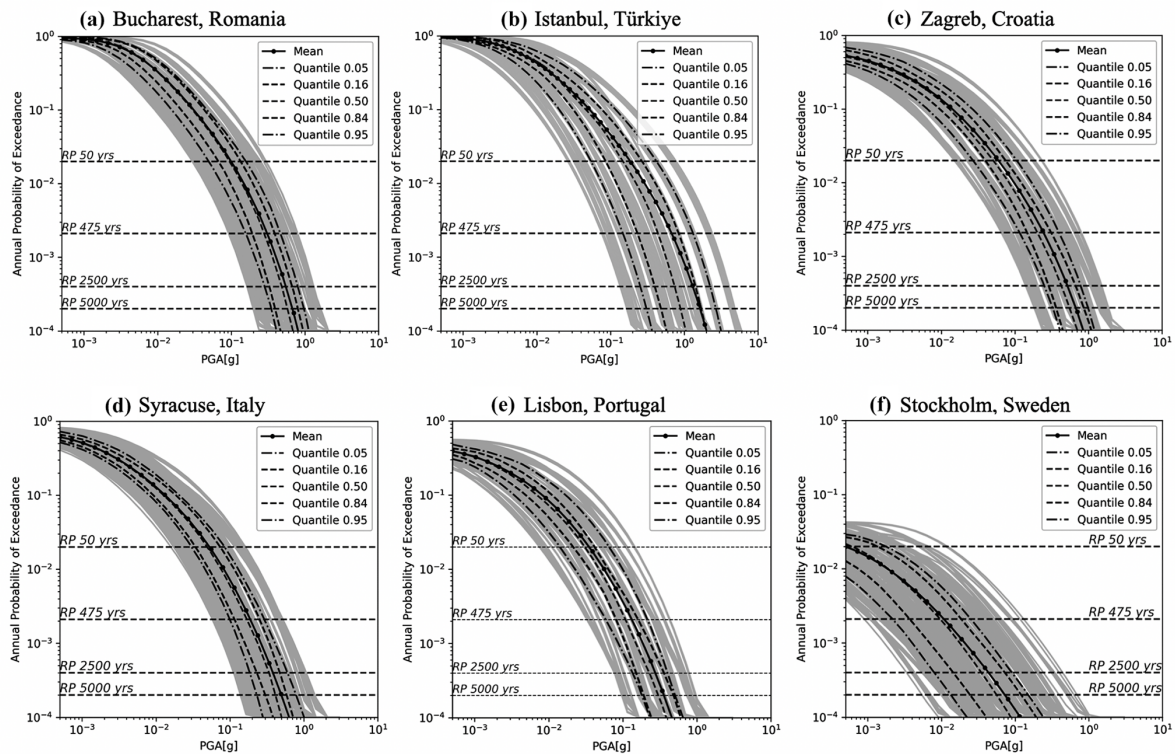


Figure 3 Hazard curves example: full distribution of hazard curves for 10 000 samples of the ESHM20 main logic tree. Mean and five quantiles (5th, 16th, 50th, 84th, 95th) are given for Bucharest (Romania), Istanbul (Türkiye), Zagreb (Croatia), Syracuse (Italy), Lisbon (Portugal), and Stockholm (Sweden). These results are applicable to generic rock soil conditions with a shear wave velocity ( $V_{s30}$ ) of  $800 \text{ m s}^{-1}$  (from Danciu et al., 2024)

**Local site evaluation** is an essential step in understanding the amplification of seismic motion induced by complex geological structures and estimating its impact on future strong earthquakes. It is a key element in hazard studies and microzoning in urban areas. Damage to infrastructure has been observed globally due to significant soil motion amplification caused by earthquakes. Quantifying these site effects in GMMs typically relies on either the average shear wave velocity up to 30 meters deep ( $V_{s30}$ , a parameter generally derived from surface geology, e.g., Allen & Wald, 2009; Thompson & Wald, 2012; Heath et al., 2020) or the soil classes defined by Eurocode 8 (CEN2004). Recent studies indicate that various site parameters, such as the fundamental frequency of resonance ( $f_0$ ; Manea et al., 2021) and the predominant frequency peak ( $f_{pred}$ ; Hassani et al., 2016), significantly contribute to describing ground variability in GMMs.

The interpretation of seismic vibrations recorded, aimed at developing a three-dimensional geophysical model of seismic velocities, represents an important step in the process of estimating seismic hazard. By analyzing ambient vibration signals as well as earthquakes recorded at a significant number of stations installed over a wide area, geophysical velocity profiles of primary and secondary waves can be obtained. One of the critical parameters for assessing amplification effects is the depth of bedrock, whose interface with soft sediments is responsible for the development of resonance phenomena. The depth of the seismic bedrock is an essential parameter that must be considered in seismic hazard evaluation, as ground motion generated by earthquakes can be significantly amplified in sediment layers where seismic wave propagation velocities are low (Baise et al., 2016; Manea et al., 2017). Identifying the depths of various geological interfaces and interpreting the results alongside available geological/geophysical data provides a comprehensive overview of the terrain.

Three-dimensional models are essential for estimating local seismic effects. The subsurface structure concerning Romania, along with seismicity data, serves as fundamental information for assessing the seismic hazard at the regional/national level. Together with local seismic effects, they provide the necessary input for seismic risk analysis.

Several studies regarding the evaluation of local response in the metropolitan area of Bucharest, located in the center of the Moesian Platform, have highlighted the importance of local geological structure alongside source properties and the propagation trajectory of seismic waves (Cioflan et al., 2004; 2009).

There are several techniques for estimating the seismic effects in local/surface geological structures generated by the propagation of seismic waves. These techniques are based on experimental methods and instrumental data (such as macroseismic intensities, noise, and recordings of weak to strong motion) or numerical modeling (e.g., finite difference, finite element methods). In these methods, the propagation medium is considered to be linear elastic, linear equivalent, infinite, or partially finite (Apostol, 2010; 2017; Mărmureanu et al., 2005).

Frequently, uncertainties arise in the spectral characteristics of relative amplitudes due to specific local conditions, source characteristics, and the propagation of the wave field through the medium. The spectral characteristics of micro-vibrations could provide some insights into local conditions for a particular area.

The Horizontal to Vertical Spectral Ratio technique (HVSR, Konno et al., 1998; Nogoshi et al., 1971; Nakamura, 1989; Poggi et al., 2012) is used as a fundamental tool for estimating seismic response on a particular site. According to these authors, HVSR curves provide not only information about the resonance period and frequency but also about the corresponding amplification. On the other hand, some authors have found that the amplification factor

determined using the HVSR technique does not fully express local amplification (as noted in the study by Field et al., 1995), which observes a tendency to underestimate compared to classical reference station methods. Additionally, interpreting the spectral ratio curves offers useful and robust information about seismic ground motion models and the seismic response of shallow geological layers (Manea et al., 2016; 2017).

Due to its low cost and fast implementation, the HVSR method has become widely used, primarily for extracting essential information about the geological structure of a site to assess local effects that arise during a seismic event. Knowing the characteristic resonance frequency of the ground allows for estimating which types of constructions are exposed to significant damage (Ohmachi et al., 1991; Balan et al., 2008), contributing to the development of strategies to mitigate the building-ground resonance phenomenon during strong earthquakes (Bratosin et al., 2017).

This method involves calculating the spectral ratio between the Fourier spectrum of the horizontal components ( $FFT_{est}(f)$ ,  $FFT_{nord}(f)$ ) and the Fourier spectrum of the vertical component ( $FFT_{vertical}(f)$ ) of the waveforms recorded by a single station equipped with a three-component sensor. The Fourier transform is computed for each seismic signal and is used to create the frequency spectrum. This technique can be applied to both ambient vibrations and recordings from seismic events. Using the above notations, it is mathematically expressed as follows:

$$\frac{H}{V}(f) = \frac{\sqrt{F_{est}(f)^2 + F_{nord}(f)^2}}{|F_{vertical}(f)|} \quad (2)$$

The method is based on the assumption that the vertical ground motion is not amplified by the surface layers; therefore, the ratio of the resultant horizontal component to the vertical component corresponds to the transfer function or seismic amplification between the seismic bedrock and the free surface (Kassaras et al., 2017). The HVSR technique is fast and efficient, widely used in microzoning studies (Lermo & Chavez-Garcia, 1993;; Ozcep et al., 2010), providing information about the geological structure that characterizes the site.

On the other side, recently recorded data in Romania during the seismic sequence of Gorj, in 2023, evidence the fact that the fundamental frequency of resonance identified in noise HVSR (NHVSR) curves is not always retrieved in seismic site response computed from records. Another important observation is that earthquake HVSR (EHVSR) exhibits high amplifications at secondary peaks of the NHVSR (Figure 4). Amplification effects at high frequencies (6 – 9 Hz) exist even for medium-magnitude events and the higher-frequency peak ( $f_i$ ) can “give” the maximum in the recorded response spectra.

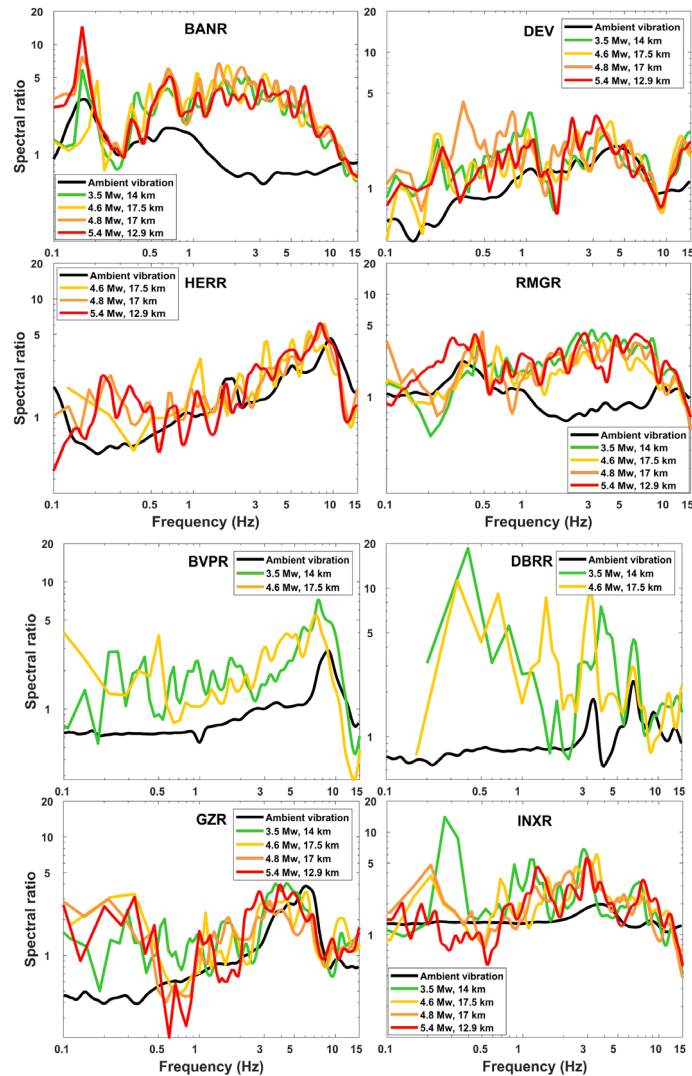


Figure 4. NHVSR and EHVSR curves for the stations located far-field (left) and close-field (right) related to earthquakes in the Gorj, Romania 2023 sequence (colored lines).

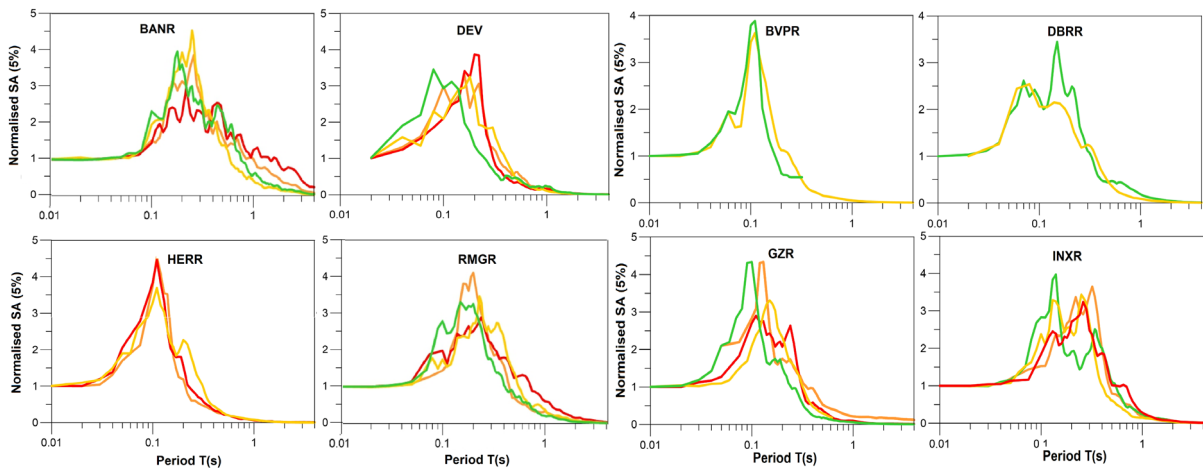


Figure 5. Response spectra for the analyzed seismic events (the colored lines are unitary as in Figure 4) for far-field (left) and close-field (right), related to earthquakes in the Gorj, Romania 2023 sequence.

Stations placed on complex geological structures having multiple NHVSR peaks exhibit similar behavior: important “amplification” in EHVS curves around  $f_0$  and  $f_1$  and highest response spectra at values ( $T_{\text{peak}} \rightarrow f_{\text{peak}}$ ) similar to  $f_1$  (DBRR  $f_1 = 6.5$  Hz,  $f_{\text{peak}} = 6.6$  Hz; HERR  $f_1 = 9.5$  Hz,  $f_{\text{peak}} = 9.1$  Hz);

In microzonation studies, depending on the characteristics of the built environment, high-frequency resonance peaks became more important and should not be neglected as the current practice does.

These findings will contribute to a better understanding of the local site effects and seismic response in the study areas, providing valuable information for earthquake engineering applications and risk mitigation strategies in the region.

## 2.2. ShakeMap methodology

Earthquakes pose significant risks to communities worldwide, necessitating rapid assessment tools to help emergency response and mitigation efforts. ShakeMap, developed by the U.S. Geological Survey (USGS) (Wald et al., 2005), is a powerful tool that integrates both observed data and predictive models to provide reliable estimates of ground motion parameters and to portray the level and distribution of the seismic ground shaking following significant seismic events, which are essential for effective emergency response.

When an earthquake occurs, the generated seismic waves are first detected by a seismic network and rapid estimation of the earthquake's magnitude and the location of its hypocenter is performed using automated algorithms. These initial parameters are essential for triggering the ShakeMap process and serve as the basis for applying Ground Motion Models (GMM) to predict ground-motion parameters, such as Peak Ground Acceleration (PGA), Peak Ground Velocity (PGV), and Spectral Acceleration (SA) in near and far field. The GMMs are selected based on specific relevance criteria, including magnitude range, fault mechanism and dimensions, distance from the source, and the geodynamic context of the region. By accounting for these factors, GMMs provide an initial estimate of the expected ground shaking across the affected area.

As the seismic waves propagate, they are recorded by seismic stations equipped with accelerometers and/or seismometers and ground motion measurements (e.g. PGA, PGV) are computed. The instrumental data are sometimes corrected for site amplification factors to revert the measurements from soil conditions to rock conditions. This correction is essential because local soil conditions can significantly amplify or deamplify seismic waves. The corrected observations are then used to update the initial ground-motion estimates provided by the GMMs. Advanced statistical techniques are used to interpolate and combine observed data with modeled predictions. This process refines the distribution of the ground-motion field, enhancing the accuracy of the ShakeMap.

In addition to instrumental data, macroseismic intensities reported by individuals are sometimes collected and converted into ground-motion estimates using Ground-Motion-Intensity Conversion Equations (GMICEs). After updating the ground-motion field, site amplification factors are reapplied at the defined grid points to adjust the ground-motion parameters from rock conditions back to the actual soil conditions of the area. This step ensures that the ShakeMap reflects the true ground shaking experienced at the surface, accounting for local geological effects.

In the end, various products are generated, including ground motion parameter maps, intensity maps and uncertainty maps. Advanced visualization techniques improve interpretability, using intuitive color scales, contour lines and annotations to effectively transmit information to end users.

The USGS ShakeMap is the most widely used shakemap tool worldwide. It is an open-source software package that can be customized by seismological agencies and researchers around the world to meet their specific regional needs, incorporating local GMMs, on-site amplification factors, and observational data. This ensures that the ground shaking intensity maps produced are accurate and relevant for different geographical areas.

Currently, there are two versions of ShakeMap software, version 3.5 and version 4, which have been implemented in many national or regional institutions around the world (e.g. in Europe: Switzerland, Italy, Greece, France, Romania, etc.). The reader can find a description of countries that have implemented ShakeMap in Annex 1.

The software versions were written in different scripting languages:

- version 3.5 was developed mainly in Perl, a scripting language that made code maintenance, extensibility and integration with modern tools difficult
- version 4.0 was developed with Python as the main programming language to overcome these problems.

Having seismic stations at each of the required grid points would be ideal. But in reality, most of these grid points do not have stations nearby, often being tens of kilometers away from the nearest station. To construct the most accurate shaking map, the mapping approach combines data from individual stations, site amplification characteristics, and ground motion prediction equations based on the distance to the earthquake source (either the hypocenter or the causative fault). The intent of this approach is to provide reasonable estimates at grid points far from the available data, while retaining detailed earthquake information where stations are nearby.

In the following, we describe the ShakeMap methodology, emphasizing the steps involved in generating the shaking maps and presenting the similarities as well as the main differences between versions 3.5 and 4.0.

### **ShakeMap essential input data**

In order for ShakeMap to produce the desired maps with the distribution of the ground motion parameters, specific seismic information is needed:

- a) Earthquake source parameters - represent estimates of the earthquake's magnitude, the hypocenter location and fault-source models, if available;
- b) Shaking intensity measures (IMs) - are quantitative measurements such as PGA, PGV and SA values at different periods from seismic stations.

Earthquake source parameters can be integrated into ShakeMap with varying levels of detail, starting from basic fault representations and advancing to detailed rupture models. Cultrera et al. (2013) examined how considering the effects of earthquake sources at different levels of detail can improve the mapping of ground shaking. They discussed several source rupture models with gradually increasing details:

- a) Point source model - at this level, the earthquake is modeled as a point source located at the hypocenter. While this simplification is useful for rapid assessments, it does not capture the spatial extent of the fault or the heterogeneity of the rupture process, potentially leading to inaccuracies in predicted ground motions, especially near the fault;

- b) Finite-fault approximation - approximate the fault as a rectangular area surrounding the epicenter. This basic geometric representation can be obtained rapidly through quasi-real-time inversion of peak ground parameters, given the known hypocenter and magnitude of the earthquake (Convertito et al., 2012; Convertito & Emolo, 2012). Studies have shown that this finite-fault approximation significantly enhances ShakeMap's performance. For instance, Moratto and Saraò (2012) demonstrated that replacing the point-source model with a finite-fault representation can reduce the misfit between computed and reference shakemaps by up to 40%;
- c) Preliminary rupture model incorporating source effects - as more data become available after a strong earthquake, the fault model can be refined to include source effects such as rupture directivity. Hours after an earthquake, preliminary slip models can be derived from the inversion of teleseismic data. Incorporating this information allows more accurate simulations of earthquakes at uninstrumented sites, further improving the reliability of ShakeMap results;
- d) Kinematic rupture model - approximately 1 day after the event, a complete rupture model can be developed by kinematic inversion of strong motion records. This detailed model captures the complex fault geometry and the nuances of rupture propagation, including variations in slip distribution and rupture velocity. By integrating this information into ShakeMap, a high-fidelity simulation of seismic motion can be obtained that closely mirrors the actual earthquake motion.

ShakeMap is designed to interact smoothly with various seismic processing systems widely used worldwide, such as Antelope (Boulder Real Time Technologies, 2007) or SeisComP3 (Helmholtz-Centre Potsdam - GFZ German Research Centre for Geosciences and Gempa GmbH). These allow data acquisition from the seismic stations that recorded the earthquake, data processing, computation of earthquake hypocentral and ground motion parameters (PGA, PGV, SA at periods of 0.3, 1.0, and 3.0 s) and transmission of the required input to the ShakeMap application in specific formats, mainly XML or JSON. The seismic data introduced in ShakeMap must be correctly formatted and include complete metadata for each station, such as location, network identification and channel information.

In areas where instrumental data are lacking, observations of macroseismic data become invaluable. ShakeMap can handle inputs in the form of observed intensities, such as the Modified Mercalli Intensity (MMI) scale. These observations often come from public reports or from traditional expert intensity assessments. One of the main sources of intensity data immediately after the earthquake is the "Did You Feel It?" system. (DYFI) system (Wald et al., 2011). DYFI collects information from public sources on earthquake intensity, which can be retrieved and formatted for input into ShakeMap.

Macroseismic intensity data are converted into estimates of ground motions using GMICE equations. These equations establish empirical relationships between observed intensities and instrumental ground motion parameters. Because GMICE involves inherent uncertainties due to regional variations and geologic conditions, ShakeMap accounts for this by negatively weighting the converted observations during the interpolation process. Macroseismic data, such as peak ground motion parameters, should be written to XML or JSON files with site metadata.

## ShakeMap v3.5

In regions where seismic instrumentation is sparse or absent, estimating ground motions after an earthquake becomes challenging. To address this problem, ShakeMap relies on earthquake source parameters and predictive models such as GMMs and Intensity

Prediction Equations (IPEs). While GMMs are widely available for various magnitudes, source mechanisms, and tectonic settings, IPEs are comparatively scarce, primarily focusing on active tectonic regions and stable cratonic environments (Atkinson and Wald, 2007; Allen et al., 2012). For this, ShakeMap 3.5 introduces a "virtual IPE", combining a selected GMM with a GMICE.

ShakeMap's main products consist of interpolated grids of ground motion parameters, from which various other products such as contours and maps are derived. These grids include parameters such as PGA, PGV, MMI and SA at 0.3, 1.0, and 3.0 s periods. The main principles of the ShakeMap workflow are described in the following and represented in Figure 1 (after Wald et al., 2005).

### **Data preparation**

Ground motion data are supplied to ShakeMap in XML format, containing measurements from various seismic stations. Each station is identified by a unique code and may have multiple channels corresponding to different instrument orientations. ShakeMap focuses on the peak horizontal components of motion, ignoring vertical components. If any amplitude in a station's input XML is flagged as problematic, e.g. the "flag" attribute is not null and not zero, then all components of that station are considered unusable. The underlying assumption is that when problems occur in a component's data stream all components derived from the same data stream are likely affected. Since the determination of a reliable peak horizontal ground motion value depends on consistent and quality data in all components, a single flagged component compromises the entire dataset from that station.

### **Converting between intensity and peak ground motions**

After reading the input data and determining peak amplitudes, ShakeMap uses GMICEs to convert between intensity measures (e.g. MMI) and peak ground motions (PGM, e.g. PGA). This bidirectional conversion allows for consistent integration of different types of observations. However, low-intensity observations (MMI less than III for PGA and less than IV for other parameters) are excluded from conversion to PGMs, as they can introduce significant errors due to the wide variability in ground motions associated with low intensities.

### **Site corrections, amplification factors and correcting data to "rock" conditions**

Soil and rock conditions significantly influence ground motions. To account for these local effects, ShakeMap first removes near-surface amplification from the observational data, effectively standardizing it to "rock" conditions. This allows more accurate interpolation in areas with different site characteristics. The Vs30 parameter serves as a proxy for site conditions and is fundamental to both GMM and site amplification calculations.

ShakeMap offers two methods for determining site amplification factors based on Vs30:

- Frequency- and amplitude-dependent factors - derived from studies like Borcherd (1994) or Seyhan and Stewart (2014), these factors adjust for site effects across different frequency bands.
- GMM-based site correction terms - utilizes site amplification terms provided within the selected GMM.

Typically, ground-motion observations are corrected (de-amplified) to rock conditions using the first method. For parameters like PGV, which are not directly handled by some amplification models, conversions to PSA at specific periods are performed for correction and then converted back, ensuring no bias or uncertainty is introduced.

### **Event bias correction**

To improve ground motion estimates, ShakeMap calculates an event-specific bias that adjusts the GMM predictions to better align with observed data. This bias correction effectively removes inter-event variability inherent in the GMM. The process involves:

- a) adjusting the earthquake magnitude to minimize the misfit between observations and GMM estimates
- b) applying directivity corrections if selected
- c) down-weighting converted observations to reflect their higher uncertainty
- d) iteratively flagging and excluding outliers beyond a specified threshold.

### **Interpolation of ground motions**

ShakeMap is built on a weighted interpolation procedure that integrates various data sources while taking into account their uncertainties. The method, detailed in Worden et al. (2012), combines direct measurements, converted observations, and predictive models to produce a comprehensive image of the intensity of earthquake ground motion. To estimate ground motion at any point of the grid, ShakeMap computes an uncertainty-weighted average of three primary data types:

- Direct measurements of the ground motion or intensity recorded directly at seismic stations (e.g. PGA);
- Converted observations - observations of one type are converted to another using GMICES;
- Predictions derived from GMPEs or IPEs based on the earthquake's source parameters,

Since the grid points where PGM estimates are needed are often at different distances from the observation sites, the interpolation needs to consider how the uncertainty increases with distance. ShakeMap uses a spatial correlation function to model this phenomenon, thus emphasizing that seismic ground motions at nearby locations are more closely related than those farther away:

- For direct ground-motion observations (e.g. PGA) the uncertainty is assumed to be zero at the observation site since they are precise measurements from instruments. However, the uncertainty increases due to spatial variability as the ground motion is estimated at points away from the station;
- For intensity observations (e.g., MMI) there is inherent uncertainty because intensity values are subjective assessments and represent averaged effects over an area rather than point measurements;
- For model estimates (GMM/IPE) the uncertainties are those specified in the models themselves, often derived from statistical analyses of seismic data. These uncertainties may vary spatially, especially in modern models that incorporate regional variations.
- For converted observations additional uncertainty arises from the conversion process between different measurement types. This conversion uncertainty, associated with the GMICE, results in converted observations being given less weight compared to direct measurements.

To account for distance differences between observations and grid points, ShakeMap adjusts each observation using a scaling factor based on the expected attenuation of ground motion with distance. This scaling ensures that the observation reflects what might be expected at the grid point, taking into account the expectations of the predictive model.

The adjusted observation  $Y_{obs,xy}$  at a grid point (x,y) is calculated as:

$$Y_{obs,xy} = Y_{obs} \times \left( \frac{Y_{GMM,xy}}{Y_{GMM,obs}} \right)$$

Where:

- $Y_{obs}$  is the observed ground motion at the station;
- $Y_{GMM,obs}$  is the model-predicted ground motion at the observation site;
- $Y_{GMM,xy}$  is the model-predicted ground motion at the grid point.

This scaling accounts for geometric factors and ensures that the adjusted observation is consistent with the expected attenuation patterns of the seismic waves.

The estimated ground motion at each grid point is then determined by combining all adjusted observations and model estimates, weighted by the inverse of their variances (uncertainties):

$$Y_{xy} = \frac{\frac{Y_{GMM,xy}}{\sigma_{GMM}^2} + \sum_i \frac{Y_{obs,xy,i}}{\sigma_{obs,xy,i}^2} + \sum_j \frac{Y_{CONV,xy,j}}{\sigma_{CONV,xy,j}^2}}{\frac{1}{\sigma_{GMM}^2} + \sum_i \frac{1}{\sigma_{obs,xy,i}^2} + \sum_j \frac{1}{\sigma_{CONV,xy,j}^2}}$$

Where:

- $Y_{xy}$  is the estimated ground motion at grid point (x,y);
- $Y_{GMM,xy}$  and  $\sigma_{GMM}^2$  are the model prediction and its variance at the grid point;
- $Y_{obs,xy,i}$  and  $\sigma_{obs,xy,i}^2$  are the adjusted observations and their variances for each direct observation i;
- $Y_{CONV,xy,j}$  and  $\sigma_{CONV,xy,j}^2$  are the adjusted converted observations and their variances for each converted observation j.

This equation ensures that data with a lower uncertainty have a larger influence on the estimated ground motion, thus complying with the principles of statistical weighting.

An important aspect of this interpolation process is that the total variance at each grid point is given by the reciprocal of the denominator in the equation. This total variance represents the combined uncertainty from all data sources contributing to the estimate at that point. It serves as a valuable metric for assessing the confidence level of the estimated ground motions across the grid.

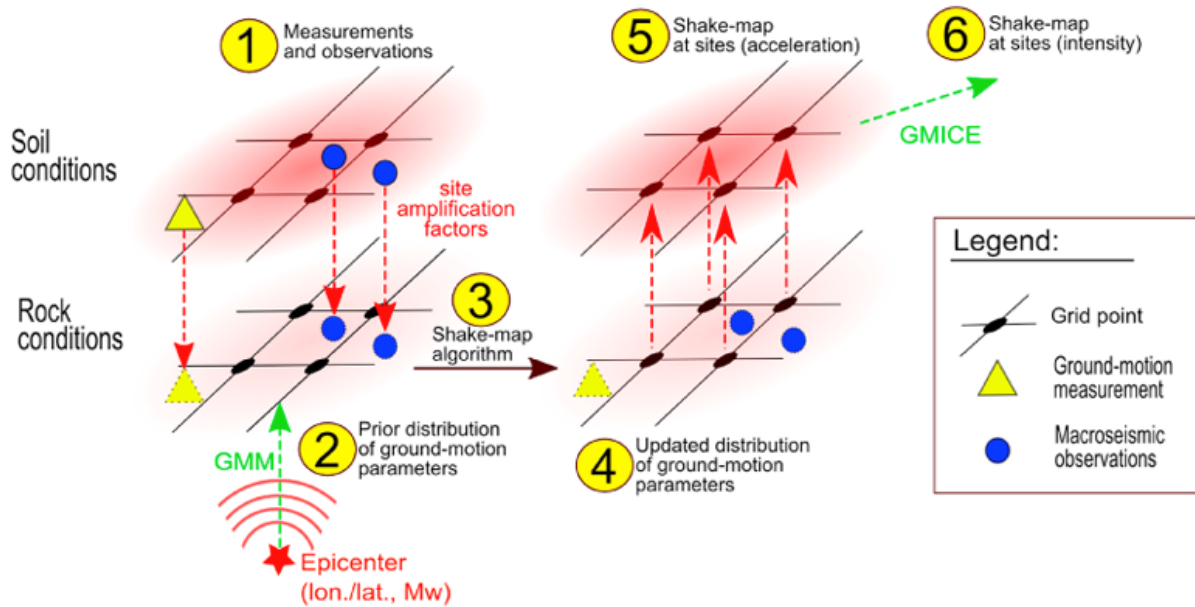


Figure 6 Schematic main principles of the ShakeMap workflow (after Guerin-Marthe et al., 2021)

## ShakeMap v4.0

The transition from ShakeMap version 3.5 to 4.0 brought several key changes in how ground motion and intensity predictions are handled. The following highlights the main differences between the two versions.

### Shift to Multivariate Normal Distribution (MVN) interpolation

One of the most significant changes in ShakeMap 4.0 is the adoption of a conditional multivariate normal distribution (MVN) approach for interpolating ground motions (Engler et al., 2022). This statistical framework allows for a more rigorous incorporation of correlations between different ground-motion intensity measures (IMTs) and accounts for spatial variability and uncertainties in a cohesive manner. The MVN approach improves the interpolation by:

- Incorporating cross-correlations that models the relationships between various IMTs (e.g., PGA, PGV) and their spatial correlations across the affected region;
- Improving uncertainty quantification by taking into account the joint probability distribution of all IMTs, the method provides more accurate estimates of the uncertainties associated with predictions of ground motion.

“The vector of ground-motion parameters  $Y$  (assumed to be normally distributed) is divided into  $Y_1$  ( $m$  prediction sites, or grid points) and  $Y_2$  ( $n$  observations sites), with the following expressions for the mean and variance:

$$\mu_Y = \begin{bmatrix} \mu_{Y_1} \\ \mu_{Y_2} \end{bmatrix} \quad \Sigma_Y = \begin{bmatrix} \Sigma_{Y_1 Y_1} & \Sigma_{Y_1 Y_2} \\ \Sigma_{Y_2 Y_1} & \Sigma_{Y_2 Y_2} \end{bmatrix}$$

Then, given a set of observations  $Y_2 = y_2$ , a vector of residuals is defined as  $\zeta = y_2 - \mu_{Y_2}$ . Thanks to the MVN, it is possible to express the mean and variance of the set of predictions  $Y_1$ , as follows:

$$\mu_{Y_1|y_2} = \mu_{Y_1} + \Sigma_{Y_1Y_2} \cdot \Sigma_{Y_2Y_2}^{-1} \cdot \zeta$$

$$\Sigma_{Y_1Y_2|y_2} = \Sigma_{Y_1Y_1} - \Sigma_{Y_1Y_2} \cdot \Sigma_{Y_2Y_2}^{-1} \cdot \Sigma_{Y_2Y_1}$$

The initial mean values of  $Y_1$  are obtained from a GMM, and the variance-covariance matrix is assembled from the standard deviations associated with the GMM and from the spatial correlation structure of the ground motion parameter(s) of interest. Therefore, the results from the previous two equations may be directly used as the updated ground-motion distribution for the generation of the shake map. Worden et al. (2018) also show that this approach enables the consideration of multiple types of ground-motion parameters (e.g., PGA, SA at different periods) simultaneously: thanks to the cross-correlation structure between some ground-motion parameters (esp. spectral responses), it is possible to gain knowledge and constrain shake-maps when only parameters of a given type have been recorded, for instance" (after Guerin-Marthe et al., 2021).

### **Enhanced GMM integration and weighting**

In ShakeMap 3.5, ground-motion predictions relied on selected GMMs appropriate for the region and tectonic setting, often using a single GMM or a simple average of multiple models. Version 4.0 introduces the MultiGMM class, which allows for a weighted combination of multiple GMMs, facilitating smooth transitions between different tectonic environments and consistency with other seismic hazard models.

Key differences include:

- Customizable GMM sets - operators can define GMPE sets with specific weights, enabling more tailored ground-motion predictions that reflect the complex nature of seismic wave propagation in various geological settings;
- Handling of model uncertainty - ShakeMap 4.0 calculates the variance of the weighted mean ground motion by considering the covariance between the GMMs, accounting for non-constant variability in the model uncertainties.

The GMMs are drawn from the set of GMMs implemented by the GEM OpenQuake software (GEM, 2024).

### **Limitations and approximations in GMICE usage**

While both versions rely on ground motion-to-intensity conversion equations (GMICE) to convert between instrumental measurements and intensity scales such as modified Mercalli intensity (MMI), ShakeMap 4.0 explicitly recognizes the limitations due to the sparsity of cross-correlation functions between different MMIs and intensities. Version 4.0 implements a two-step process in which conversions are performed with caution, and the uncertainties associated with these conversions are explicitly accounted for and used to reduce the weight of converted IMTs during interpolation. This approach improves the reliability of intensity predictions by properly accounting for the increased uncertainty resulting from the conversions.

### **Cross-correlation Functions**

ShakeMap 3.5 did not explicitly address the lack of cross-correlation functions for certain IMTs. ShakeMap 4 handles the spatial cross-correlation among various IMTs - particularly those for which no published cross-correlation models currently exist. ShakeMap's cross-correlation computations primarily rely on the relationships defined by Loth and Baker

(2013), who provided functions specifically for spectral accelerations (SAs) at various periods. Because not all IMTs used in ShakeMap have corresponding cross-correlation models, ShakeMap makes approximations to map these other IMTs to “equivalent” SA periods: i) PGA is approximated as spectral acceleration at 0.01 seconds ii) PGV and MMI are approximated as spectral acceleration at 1.0 second.

### ***Refined outlier detection and handling***

ShakeMap 4.0 introduces a more refined approach to outlier detection compared to version 3.5. Outlier flagging is performed on a per-IMT basis, meaning that if an observation for one IMT at a station is flagged as an outlier, it does not automatically affect other IMTs at the same station unless they also exceed the deviation threshold. Additionally, ShakeMap 4.0 allows for the suspension of outlier flagging for large-magnitude earthquakes without a finite rupture model. This consideration acknowledges that predictions are less reliable without detailed source information, and observed data should not be discarded solely based on deviations from model predictions.

### ***Improved support for site amplification and Vs30 mapping***

In both versions, v3.5 and v4.0, site effects are accounted for using Vs30. ShakeMap 4.0 builds upon the methods of version 3.5 by:

- Supporting Vs30-based amplification in GMMs - with modern GMMs often incorporating Vs30 directly, ShakeMap 4.0 relies on this to apply site corrections more consistently;
- Introducing generic amplification factors - for situations where basin depth parameters are not available, version 4.0 allows for the application of user-supplied generic amplification factors to account for basin or topographic effects. These factors provide an intermediate solution until more detailed basin models can be incorporated.

### ***Event bias calculation***

Version 4.0 adopts a non-iterative approach within the MVN framework, as described by Engler et al. (2022). This method properly handles varying between-event standard deviations, improving the accuracy of bias estimation. The bias term is derived mathematically based on the size and number of residuals, allowing for bias calculation even with a single observation. This change increases the statistical accuracy of the bias estimation process and ensures that ground motion predictions are properly corrected.

### ***Challenges and uncertainties in ShakeMap generation***

Finally, it is important to summarize the challenges and uncertainties in ShakeMap generation. This is essential because it ensures that users - such as researchers, emergency responders, engineers, and policymakers - understand the limitations and credibility of the data on which they rely. By clearly communicating where uncertainties (e.g., poor station data, modeling assumptions, or complex geologic conditions) come from and what their implications are, stakeholders can make better-informed decisions, correctly assess risks, and allocate resources effectively in response to an earthquake.

While the ShakeMap methodology is robust, several challenges and uncertainties affect its accuracy and reliability:

1. Earthquake parameters estimation

- a. Initial uncertainty - immediately following an earthquake, the epicenter, magnitude, and especially depth often carry significant uncertainties. Early estimates rely on limited data, which can distort early ground-motion assessments. Accurately determining earthquake depth is critical for understanding near-field ground motions. Shallow earthquakes can produce more intense local shaking, and any error in depth estimation translates directly into inaccuracies in predicted ground shaking.
2. Selection of GMMs and GMICES
  - a. Model specificity - different tectonic settings require specialized GMMs calibrated for local seismic conditions. Using a generic or inappropriate model can yield substantial errors in predicted shaking levels;
  - b. Bias in conversion - translating instrumental ground-motion metrics (e.g., PGA) to felt intensities through GMICE introduces uncertainty. These conversion models rely on empirical relationships that may not be universally applicable.
3. Fault Mechanism and rupture dimensions
  - a. Complex rupture modeling - in the case of large earthquakes, the spatial distribution of fault slip is crucial to accurately map shaking patterns. However, obtaining a detailed finite-fault source model can take hours, during which initial ShakeMaps rely on simplified point-source assumptions;
  - b. Underestimation of fault complexity - early ShakeMaps cannot account for heterogeneous slip distributions or rupture directionality, potentially misrepresenting areas of intense shaking.
4. Site Amplification and soil classification
  - a. Local site effects - ground shaking can vary dramatically depending on local geological conditions. If the soil amplification maps (Vs30) or soil classifications are not adequately retrieved, areas with significant amplification may be underestimated or overlooked. High-quality geophysical surveys and site-specific measurements can greatly reduce uncertainties. However, such data are often limited, and relying on generalized or outdated soil classifications increases ShakeMap errors.
5. Uncertainties in GMICE and Site Amplification Factors:
  - a. Multiple conversion steps - each step in translating from rock-based ground motion predictions to felt intensities and then incorporating site effects introduces another layer of uncertainty. Continuous refinement of GMICE equations, as well as better quantification of site amplification factors, can enhance the reliability of intensity estimates derived from observed or predicted ground motions.
6. Selection of Seismic Stations for Bias Computation:
  - a. Station quality and coverage - the set of seismic stations used to adjust ShakeMaps must be carefully selected. Outlier stations or those not representative of local conditions can bias calculations. Defining which stations to include (e.g., maximum distance from epicenter, tolerance for deviation from GMPE-based estimates) affects the final ShakeMap. Too conservative criteria may eliminate valuable data, while permissive criteria may include noisy or unreliable measurements.

### 2.3. Damage and loss estimation methods

Recent terminology in seismic risk makes a clear distinction between what was previously used with similar purposes: **damage versus loss**.

**Earthquake damage** refers to the physical harm and destruction caused to buildings, infrastructure, and the natural environment as a result of seismic activity, such as ground shaking, surface rupture, and other earthquake-triggered hazards. The extent of earthquake damage depends on factors such as the earthquake's magnitude, depth, location, distance from the epicenter, local geology, building design, and preparedness measures in place. Earthquake damage can be categorized into various types, including:

- **Structural Damage:** involves damage to the load-bearing elements of a building or infrastructure, which directly affect its stability and integrity. These elements are responsible for supporting the building's weight, resisting external forces (such as wind or earthquakes), and ensuring the building's overall safety. Key Components of Structural Elements: Foundation, Load-bearing walls, Beams, Columns, Slabs, Roof structure.
- **Non-Structural Damage:** refers to damage to the interior or exterior elements of a building or infrastructure that do not contribute to the load-bearing capacity. While non-structural damage may cause operational disruptions, it does not typically pose an immediate threat to the building's overall stability or safety. Key Components of Non-Structural Elements: Partitions, infill and interior walls, Windows and doors, Ceiling finishes, Floor coverings, Electrical systems, Plumbing systems, Heating, ventilation, and air conditioning systems, Furniture and equipment.

On the other side, **losses** refer to the impact of damage. Based on the metric evaluated, losses can refer to:

- **Social Impacts:** Casualties, People displaced, Loss of services (e.g., access to healthcare, education, or utilities), Vulnerable Populations, Impact on quality of life or mental health
- **Functional Disruption:** Power outages, Transport disruptions (e.g., road or bridge collapse), Water supply and sanitation failures.
- **Recovery Time:** the time to restore infrastructure, buildings, and services, the time to return to normal economic and social conditions.
- **Economic impacts:** Repair and replacement costs, Relocation costs, Revenue losses (Business interruptions), Insurance payouts, Costs of recovery and rehabilitation, Reduced economic productivity, and Supply chain disruptions.

Both damage and losses can be:

- **Direct:** an immediate consequence of the earthquake, without needing to be inferred or linked to other factors.
- **Indirect:** secondary effects of the earthquake, like lost income or business opportunities that result from the primary damage.

In order to assess the damage, fragility functions are generally used; losses are determined afterward through consequence functions. Losses can be computed also directly, using vulnerability functions. Both fragility and vulnerability functions are tied to an intensity measure relevant to the shaking level (at ground level or within the structure). These functions are discussed in more details.

## Fragility functions

Fragility functions describe the probability of reaching or exceeding a set of limit states, given an intensity measure level. When the asset category concerns structures (e.g. buildings), the intensity measure can either be structure-independent or structure-dependent (GEM, 2024). The former can be calculated directly from recorded measurements of ground shaking (e.g. peak ground acceleration, peak ground velocity, spectral acceleration at a given period of vibration, or even macroseismic intensity). The latter requires information on the characteristics of the structures to be calculated, for example, spectral acceleration at the fundamental period of vibration, or spectral displacement at the limit state period of vibration. Fragility functions can be defined in a discrete way by providing, for each limit state, a list of intensity measure levels and respective probabilities of exceedance, or as a continuous function. Fragility functions typically define a set of discrete **damage states**, such as:

- **No damage:** intact structure
- **Minor damage:** cosmetic or non-structural
- **Moderate damage:** significant but repairable
- **Severe/extensive damage:** damage that can make the structure unsafe
- **Collapse:** failure of the structure – partially or totally.

These damage states represent different levels of deterioration or failure a structure can experience under different levels of seismic intensity. The fragility function correlates the seismic intensity measures (e.g. peak ground acceleration, velocity or displacement or spectral acceleration at different periods) with the probability of reaching a given damage state. Fragility functions are usually expressed as cumulative distribution functions (CDF) or probability density functions (PDFs) that show the likelihood of reaching a certain damage state given a specific seismic intensity.

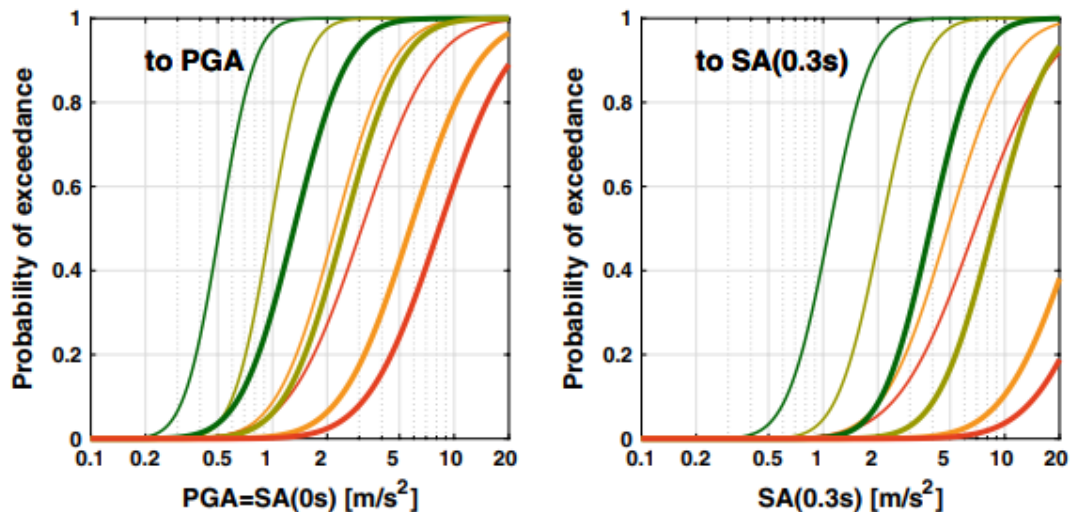


Figure 7. Fragility curves for masonry (thin lines) and reinforced concrete (thick lines) building typologies converted to PGA (left) and Sa(0.3s) (right) (Michel et al., 2018)

For the assessment of individual buildings, structure-dependent intensity measures can be utilized, as information regarding the structural characteristics, such as the fundamental period of vibration, is available a-priori. Following an earthquake, actual intensity measures (e.g., PGA, PGV, spectral ordinates) can be applied as input data, and, with the use of corresponding fragility functions, the probability of experiencing or exceeding a specific damage state can be determined.

The main methods to derive fragility functions are:

#### a) Empirical approaches

Empirical methodologies are based on the study of statistical results of actual observed damages of assets (i.e. buildings, bridges, lifelines etc.) exposed to past earthquakes. Fragility functions can be expressed in the form of damage probability matrices or tables of mean values and standard deviations of loss for each level of excitation. When reliable extensive damage data are available, empirical vulnerability functions are considered highly credible since they are derived from observations of the actual performance of assets in real seismic events. On the other hand, empirical approaches can have some important drawbacks (Porter, 2020):

- Several building types may have not yet experienced strong motion (especially new buildings);
- Extensive damage data are not available for high levels of excitation, where high losses are most likely, due to the rarity of such events;
- Available data can be heterogenous, the sample may not be representative of the building stock, inadequate inspections of buildings may have not revealed the actual damage;
- Actual loss data (in economic terms) can be hard to collect either from construction permits or insurers;

- It is difficult to estimate the ground shaking level at the observations (macroseismic intensity values are sometimes being used which also involve damage in their definition);
- Small or poor-quality databases can lead to misleading results.

### **b) Expert judgement**

In cases where no empirical data is available or the assets are difficult to model, the opinion of experts is required to provide an estimation of vulnerability quantities (e.g. mean loss, damage probability etc.). Expert opinion can be very efficient, capable of producing a new vulnerability function at the cost of a few person-hours each and of estimating the performance of buildings that have not yet experienced strong motion. Expert approaches can be grouped into two main categories: mathematical and behavioral. The first mathematically combines the answers of several experts who have no interaction with each other, while the latter aims at producing some type of group consensus among experts, who are typically encouraged to interact with one another and share their assessments (Maio & Tsionis, 2015). The major disadvantages of expert judgement approaches relate to the subjectivity of their opinions, the influence of dominant personalities and the tendency to reach speedy conclusions.

### **c) Analytical methods**

Analytical methods are based on the estimation of damage distributions through the simulation of an element's structural response subjected to seismic action. They are widely used to provide insight where empirical methods cannot (new buildings, high intensities, effects of special building properties such as soft-storey conditions, the infill panels configuration etc.). Seismic input can be represented by a response spectrum (static methods) or an acceleration time-history (dynamic methods). Numerical models need to be developed (when fragility functions are not derived through fully analytical approaches) and a compromise must be made between the accuracy of the representation of the nonlinear behavior and the robustness and cost-efficiency of the model (Rossetto et al., 2014).

The major problems of analytical methodologies are the computational cost (especially in the case of time-consuming non-linear dynamic time-history analyses) and the lack of validation by earthquake experience and/or experimental tests.

Apart from the analysis method distinctions between analytical approaches can relate to the modelling of structural (i.e. distributed plasticity or concentrated plastic hinges) and non-structural elements (e.g. infill panels), the choice between more realistic 3D models or less time-consuming 2D representations (or even single degree of freedom oscillators in some cases), the selection of the intensity measure (PGA,  $S_d$ ,  $S_a(T)$ , etc.), the selection of appropriate damage index models, the probability distribution model and the associated uncertainties, etc. An extensive review of analytical approaches for the derivation of fragility curves has been presented by Maio & Tsionis (2015).

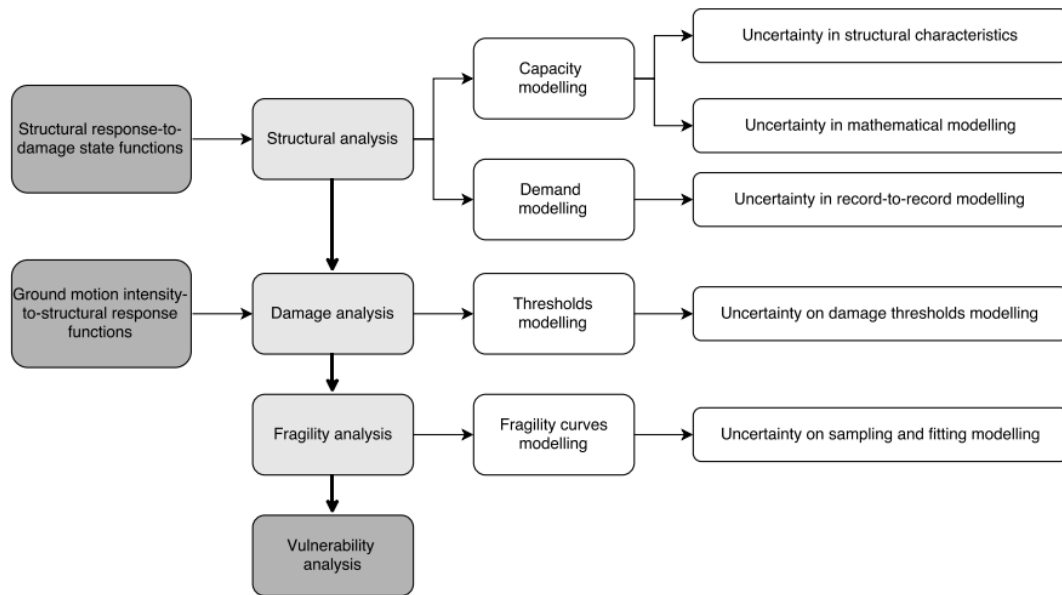


Figure 8. Main components and phases considered in analytical fragility assessment methodologies and associated uncertainties (Maio & Tsionis, 2015)

Some of the available mechanics-based vulnerability assessment methods are DBELA (Displacement-Based Earthquake Loss Assessment; Crowley et al., 2004) and SP-BELA (simplified displacement-based method; Crowley et al., 2008) – both considering that the nonlinear response of a reinforced concrete structure can be obtained from a nonlinear static analysis of the structure.

#### d) Hybrid approaches

It is possible to combine two (or more) of the aforementioned techniques for the derivation of vulnerability models, an approach that is usually referred to as “hybrid”. The need to develop such methodologies arises from limitations of each of the previous approaches, for example, the lack of empirical damage data for several building typologies or for high levels of input motions, or the lack of validation for analytically estimated results. A combination between analytical, empirical and expert opinion was presented by the EERI-WHE group within the PAGER project, attempting to define the proportion of collapses for building typologies given a shaking intensity expressed in EMS-98 Intensity for several nations worldwide. A comparative analysis of building types has been carried out and then a comparison of analytically or empirically derived curves by national studies (Pomonis et al., 2009).

#### Consequence functions

These are mathematical models or relationships used to quantify the direct and indirect consequences of a hazard (such as an earthquake, flood, or wildfire) on a system or society. They describe the probability distribution of loss, given a performance level. For example, if the asset category is buildings and the performance level is significant damage, the consequence function will describe the mean loss ratio, coefficient of variation and probability distribution for that level of damage (Figure 9). Consequence functions can be combined with fragility functions to produce vulnerability functions.

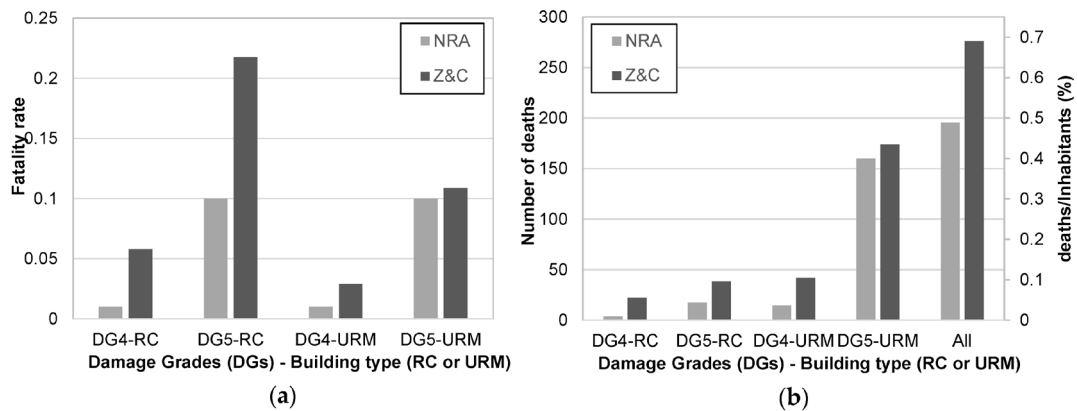


Figure 9 Fatality rates (a) and estimated number of casualties (b) as a function of damage level and building type related to the DB L'Aquila urban area for two models: NRA and Z&C (from Manfredi et al., 2023).

## Vulnerability functions

Vulnerability functions can be used to directly estimate fatalities and economic losses due to physical damage. Vulnerability functions can be continuous (Figure 10 or Figure 11) or discrete, the latter being described by a list of intensity measure levels and corresponding mean loss ratios (the ratio of mean loss to exposed value), associated coefficients of variation and probability distributions. The uncertainty on the loss ratio can follow a lognormal or Beta distribution.

For computing casualty estimates (deaths or injuries) or the number of people to be relocated, occupancy criteria are needed. These can depend on building function (residential, etc.), time of the day (day, night, commuting hours), day of the week etc. – determining occupancy rate at a specific moment (Figure 12).

Economic losses can be computed for structural and non-structural components, but also as direct losses (based for example on reconstruction values) or indirect losses (evaluating business interruption impact).

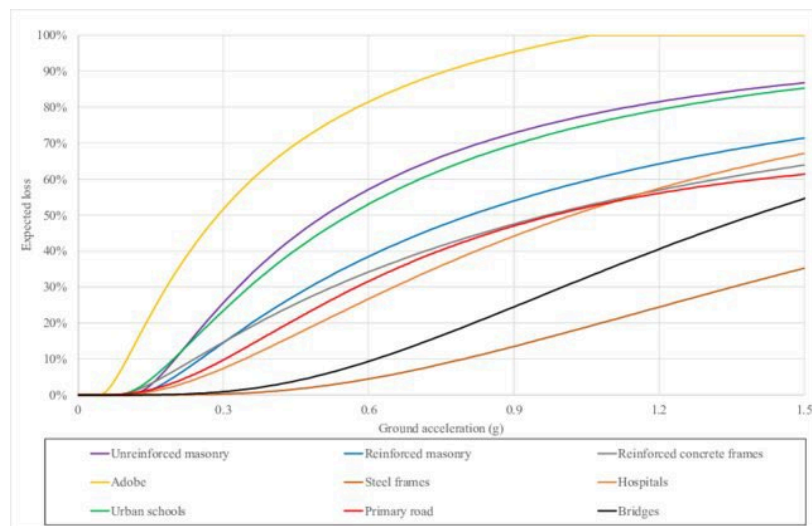


Figure 10 Example of earthquake vulnerability functions for Central Asian residential buildings and infrastructure assets (from Salgado-Gálvez et al., 2024)

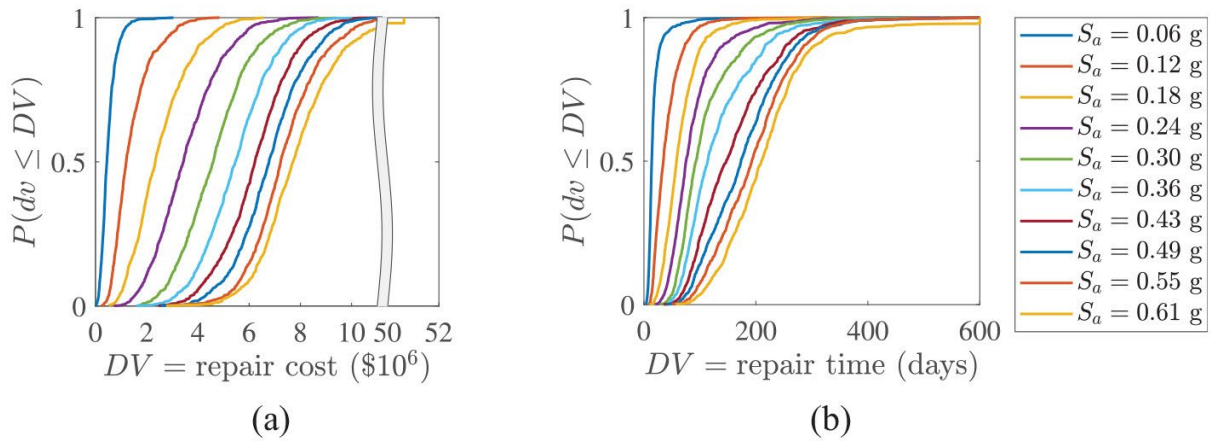


Figure 11 Cumulative distribution function of (a) repair cost and (b) repair time (from You et al., 2023)

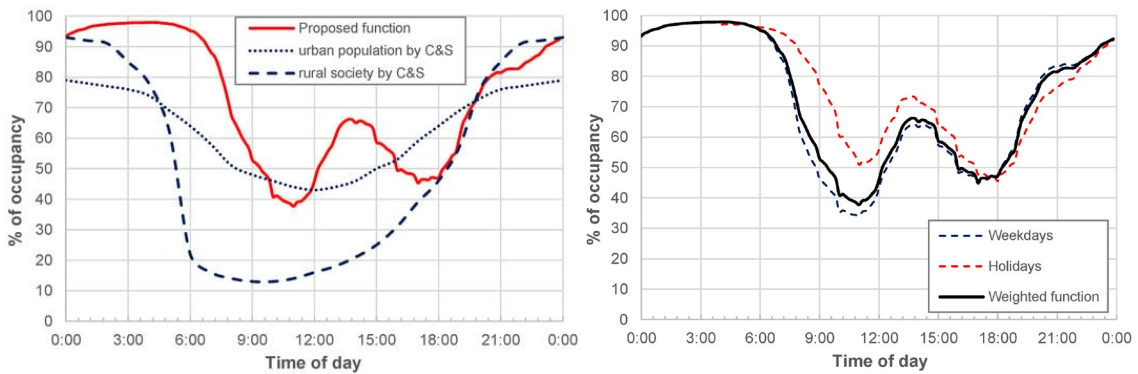


Figure 12 left) Comparison between the OR function as proposed by Coburn and Spence (2002) (for urban population, dotted blue line, and rural population, dashed blue line) and that proposed by the authors of the present paper; right) Occupancy rate function for weekdays (dashed blue line, only weighted over the municipality size) and holidays (dashed red line, only weighted over the municipality size). The solid black line refers to function weighted over the number of weekdays and holidays in one year. (from Manfredi et al., 2023)

## Databases for fragility and vulnerability functions

In literature there are many fragility and vulnerability functions available – some very specific and some more general (for a broader category of typologies). Beside multiple articles available on this topic, there are also database compilation initiatives, among which:

- The GEM Global Vulnerability Models: Martins and Silva (2023), Yepes-Estrada et al. (2016)
- Physical fragility and vulnerability models that are being used in the European Seismic Risk Model 2020 (ESRM20), accompanied by an interactive viewer: Romao et al. (2021)
- The TURNKEY Project deliverables: Tiganescu et al. (2022), D’Ayala et al. (2021)
- ReLUIS-DPC RINTC Database of fragility functions: Chioccarelli and Iervolino (2024)
- SYNER-G: Typology Definition and Fragility Functions for Physical Elements at Seismic Risk: Pitilakis et al. (2004)
- HAZUS functions: FEMA (2003)

## Structural typologies and exposure modelling

The form and parameters of a fragility function can depend on several factors of a structure:

- **Function** (e.g., residential, commercial, industrial, hospital, school)
- **Construction materials**, both for the structural system and the walls (e.g., steel, concrete, wood, adobe, masonry)
- **Structural system** (e.g., moment-resisting frame, dual frame, precast)
- **Age of the structure**, representative of seismic design codes
- **Quality of construction**
- **Previous damage or deterioration**, also with regards to structural interventions such as retrofitting
- **Height or number of floors**
- **Knowing also the number of occupants, assets and their value or floor surface is also relevant for consequence modelling and estimating losses**

Here, the role of proper exposure modelling and correspondence with fragility functions became vital. Many times, modelling a structure as detailed as possible might mean that the fragility function will be irrelevant to apply to generally similar structures. Variability from one constructor to another, from a region to another, and from a country to another imposes significant restrictions and uncertainties in using literature-based fragility functions. More generic fragility functions (such as Martins and Silva, 2023) can satisfy the purpose of seismic damage and loss estimation at a larger scale. However, applying such fragility functions at an individual building level will be highly irrelevant.

There is also significant uncertainty in exposure modeling, as more detailed information regarding the structures (such as the ones mentioned above) is many times difficult to find. Remote sensing can help to some extent, especially in determining building footprint and height.

Within the MULTICARE Project, a consistency in the definition of typologies (called also archetypes in different contexts), with regards not just to earthquake engineering aspects, is being followed, in the Work Stream 3: Multi-hazard resilience and sustainability assessment, design.

## 2.4. Triggered hazard analysis

When assessing earthquake risk, there are multiple Earthquake-Triggered Hazards (Table 2) that are highly relevant to include in the analysis, as they can be more damaging than the results of the initial shaking (especially on built structures). Some of these multi-hazards, such as liquefaction, tsunamis, landslides, or aftershocks started to be evaluated by RSLE tools. But further necessary improvements are much needed.

Table 1. Summary of Key Earthquake-Triggered Hazards

Hazard	Description	Potential Impacts
Ground Shaking	Shaking caused by seismic waves.	Structural damage, ground rupture, landslides.
Surface Rupture	Displacement along the surface fault.	Damage to buildings, roads, utilities, and pipelines.
Landslides	Movement of soil and rock due to ground shaking.	Damage to infrastructure, burial of buildings, blocked roads.
Liquefaction	Soil behaves like a liquid during shaking, especially in saturated sandy soils.	Failure of foundations, tilting buildings, damage to utilities.
Flooding	Flooding caused by landslides, dam failures, or altered riverbeds.	Submersion of properties, loss of life, environmental damage.
Tsunamis	Large ocean waves triggered by underwater earthquakes.	Coastal flooding, destruction of infrastructure, loss of life.
Seiche	Oscillations of water bodies like lakes or reservoirs.	Flooding of nearby areas, destruction of waterfront infrastructure.
Fire	Fires triggered by ruptured gas lines, electrical failures, and structural damage.	Widespread fires, property destruction, difficulty in firefighting.
Ground Deformation	Changes in the ground's elevation due to seismic activity.	Damage to buildings, roads, and agriculture.
Aftershocks	Smaller earthquakes following the main earthquake.	Additional damage and triggering of other hazards

Various RSLE software and services have started including modules for estimation of:

- liquefaction potential: OpenQuake (GEM, 2024); USGS (2024a - Figure 13)
- landslides: REDACT Project software: Papatheodorou et al. (2023); USGS (2024a) Zhang et al. (2024).

Many times, the earthquake input parameters are the ones which can be provided by ShakeMap (PGA, PSA, PGV, PGD, Intensity) or standard processing of seismic data.

Concerning aftershock forecast, there are important recent progresses (USGS, 2024b; Hardebeck et al., 2024), but this will not be the focus of the MULTICARE Project – although stakeholders revealed their interest in this information.

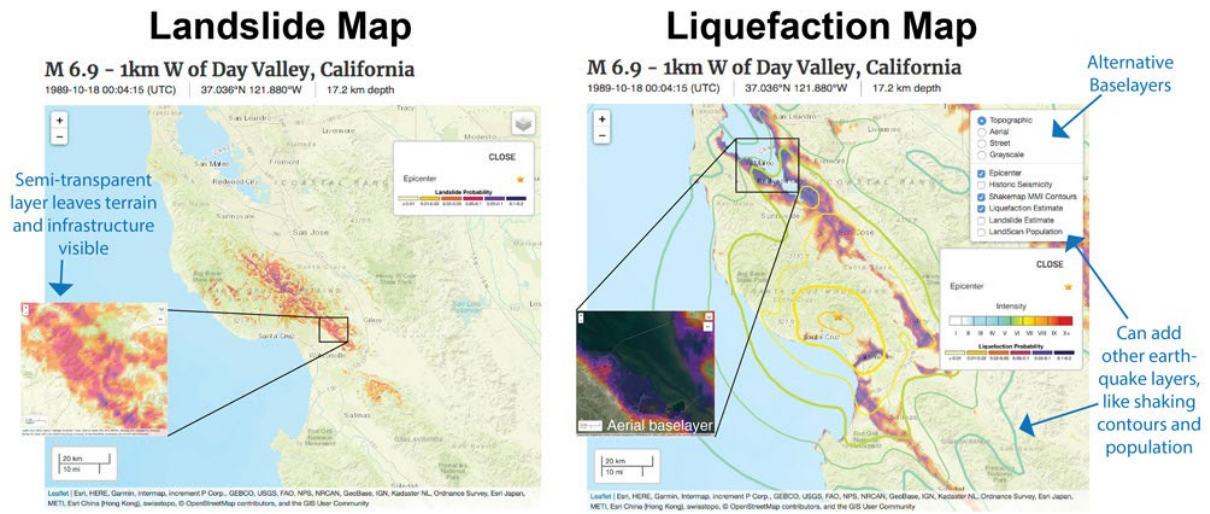


Figure 13. Screenshots of interactive map for the Loma Prieta earthquake for landslide hazard (left) and liquefaction hazard (right). Insets show zoom-in on the area indicated. (source: USGS, 2024a)

## 2.5. Overview of RSLE software available

Table 2. Comparison of software capable of RSLE implementation (in alphabetical order)

Software or system name	Owner or operator	Licensing type / modifiable	Methods	Hazard input	Exposure and vulnerability input	Outputs and their format	Areas where it was applied and at which scale	Website or references
<b>AFAD-RED</b>	AFAD (Turkey)	Not open source, written in VB-Net, C# environment and Arc-Object	Its methodology is mostly similar to HAZUS; it relies on fragility functions for various types of structures.	Preliminary results are automatically generated after receiving earthquake source parameters (epicenter, depth, magnitude) using attenuation relationships at $V_{s30}=760$ m/s then applied soil amplification according to the $V_{s30}$ database. The output is as PGA, PGV and	Loss estimations are computed using building fragility functions and consequence models. A HAZUS-based damage to Loss Model for development of Vulnerability Model can be used for determining loss ratio.  It also provides a rapid and brief representation of seismic damage and loss evaluation for bridges. The	Standard and GIS maps	Turkey; a custom version of AFAD-RED was developed within the REDACT Project and implemented in the Black Sea Crossborder Area (Papatheodorou et al., 2023)	<a href="https://depre.m.afad.gov.tr/content/91">https://depre.m.afad.gov.tr/content/91</a>  <a href="https://www.reduct-project.eu/">https://www.reduct-project.eu/</a>

				<p>Intensity maps. Different GMPEs can be selected as a weighted average. Moderate results include Fault type, length and azimuth parameters into the calculation of expected hazard level. Advanced Results include recorded ground motion analysis where first calibration is applied to estimate the recorded ground motion at <math>V_{s30} = 760</math> m/s, then the calibration of ground motion</p>	<p>vulnerability of transportation systems can be performed by choosing seven different intensity measure parameters: PGA, PGV, PGD, <math>S_d</math>, Intensity, <math>S_1</math> and <math>S_2</math>, and defining a specific fragility functions.</p>			
--	--	--	--	---	---	--	--	--

				parameter maps is performed, and the soil amplification is applied to get the resulting final PGA, PGV, spectral acceleration (SA @ 0.2 sec, SA @ 1 sec), spectral displacement (SD) and Intensity maps.				
<b>Armagedo m</b>	BRGM		Structural damage estimation: - Level 1: empirical method (namely LM1 in RISK-UE), derived from the work of Giovinazzi and Lagomarsino - - Level 2: analytical method similar to HAZUS 99 where each building class is assigned a capacity curve and the capacity spectrum method is used.	ShakeMap or scenarios	Building typology is inspired by the EMS-98 classes and refined with sub-typologies.	Collapsed dwellings and injuries	France (used in the SEISAID system)	Sedan et al (2013)

			Socio-economic losses: - consequence models					
<b>CAPRA software collection</b>	ERN-AL Consortium for the World Bank, the Inter-American Development Bank and the UN-ISDR, Universidad de los Andes (Colombia), CIMOC (Research Center on Materials and Civil Infrastructure)	Open Source Apache 2.0 License  Program ming language: Visual Basic, Requirements: MS .NET Framework	Probabilistic loss assessment algorithm: expected loss and variance calculation based on hazard analysis and vulnerability functions.	Probabilistic (using CAPRA-EQ or CRISIS2007, capable also of tsunami hazard assessment), accounting also for local site effects using SEISMIC HAZARD INTEGRATION or SOIL EFFECTS CAPRA modules	- *.shp files with certain formatting requirements for exposure; - estimation of direct losses by means of vulnerability functions (can be defined using FUNVUL Simplified, ERN Vulnerability or FUNVUL Components CAPRA modules); can be provided in *.ASCII or *.xml format.	- Expected Loss and variance calculation, Loss probability distribution function calculation for the event and Loss exceedance rate calculation using the loss PDF associated to each event and its occurrence frequency.  Output format: - Text file *.res containing for each scenario analyzed the expected loss (EP), the variance of the loss (VarP), · Excepted annual damage per building, annual human loss per building in *.shp file and viewed as a map	Central and South America and in some countries of Europe, Africa and Asia.	<a href="https://ecapra.org/">https://ecapra.org/</a>

<b>ELER</b>	NERIES Project	Free download, written in Matlab but code not shared	<ul style="list-style-type: none"> <li>- Level 0: similar to PAGER system of USGS</li> <li>- Level 1: intensity based empirical vulnerability relationship is employed to find number of damaged buildings. The casualty estimation is done through number of damaged buildings.</li> <li>- Level 2: spectral acceleration-displacement-based vulnerability assessment methodology is utilized for the building damage estimation. The casualty estimation is done through number of damaged buildings using HAZUS99 and HAZUS-MH (2003) methodologies</li> </ul>	<ul style="list-style-type: none"> <li>- Level 0 and 1: intensity distribution (ShakeMap or included IPE)</li> <li>- Level 2: ShakeMaps or custom ShakeMap module with different GMPEs included</li> </ul>	<ul style="list-style-type: none"> <li>- Level 0: population distribution (Landscan data included);</li> <li>- Level 1: EMS98 Intensity based building vulnerability with uncertainties and casualty distribution;</li> <li>- Level 2: capacity and fragility functions, distribution of population per building typologies, replacement cost and loss ratio related to damage states and pipeline location and typologies</li> </ul>	<ul style="list-style-type: none"> <li>- Level 0: estimates the number and distribution of casualties;</li> <li>- Level 1: calculates number of damaged buildings and associated casualty;</li> <li>- Level 2: also calculates number of damaged buildings and associated casualty.</li> </ul>	Turkey (especially Istanbul)	<a href="https://ege.boun.edu.tr/en/eler-tool">https://ege.boun.edu.tr/en/eler-tool</a>
<b>EQIA (Earthquake Qualitative Impact Assessment)</b>	EMSC		An impact estimate is carried out for all earthquakes of magnitude 5 or more, with a hypocentral depth of less than 150 km and for which a	Up to magnitude 7, EQIA is based on a point-source approximation. Beyond M7,	EQIA is able to quickly detect a potentially damaging earthquake, depending on its magnitude and	Results are expressed in terms of expected fatalities (with mean value and uncertainty range)	Euro-Mediterranean Region	Guerin-Marthe et al. (2021); Julien-Laferrière (2019)

			non-negligible part of the population was exposed to a shaking level of at least 0.05g, an estimate based on a Ground Motion Predictive Equation.	6 scenarios are calculated, 3 for each nodal plane of the moment tensor, 2 unilateral ruptures and one bilateral.	on the density of population in the affected region.			
<b>HAZUS</b>	FEMA, USA	Free but runs with ESRI ArcGIS	<p>Hazus is designed to support two general types of analysis (Basic and Advanced) split into three levels of data updates:</p> <ul style="list-style-type: none"> <li>- Levels 1: default hazard, inventory and damage information. The effects of possible liquefaction and landslide hazards are ignored.</li> <li>- Level 2: combination of local and default hazard, inventory and damage data.</li> <li>- Level 3: input detailed engineering data.</li> </ul> <p>For the evaluation of damage to buildings and essential facilities, a standardized response spectrum</p>	<p>Probabilistic or deterministic (includes GMPEs mostly specific to US). Hazard module account for soil characteristics, including site classification according to the National Earthquake Hazard Reduction Program (NEHRP). Can also perform induced liquefaction, landslide and</p>	<p>The Hazus Earthquake Model comes with a large library of baseline nationwide inventory data, which can be updated with local data to increase the accuracy of the model. For most elements, capacity and fragility functions are used, as well as consequence or vulnerability functions for loss estimation purposes.</p> <p>Hazus integrates local inventory data including</p>	<ul style="list-style-type: none"> <li>- Ground Motion Descriptions/Maps</li> <li>- Direct Physical Damage – General Building Stock: Structural and nonstructural damage state probabilities; cost of repair or replacement; Loss of contents; Business inventory loss; Relocation costs; Business income loss; Employee wage loss; Loss of rental income.</li> <li>- Direct Physical Damage – Essential facilities: Structural damage state probabilities by facility; Expected functionality at Day</li> </ul>	USA, Cairo (Egypt)	<a href="https://www.fema.gov/hazus-software">https://www.fema.gov/hazus-software</a>

		<p>shape is used, relying on PGA and SA values, as well as capacity, fragility or vulnerability functions.</p> <p>All details can be found in the Hazus Earthquake Model Technical Manual.</p>	<p>tsunami analysis (Potential Earthquake Hazards). For the analysis of building damage, three ground motion parameters are used: PGA, SA at 0.3 seconds, and SA at 1.0 second. PGV is used in the analysis of pipeline damage.</p>	<p>essential facilities, system, general building stock, user-defined facilities, or Advanced Engineering Building Model (AEBM) structures.</p>	<p>1, 3, 7, 14, 30 and 90 by facility.</p> <ul style="list-style-type: none"> <li>- High Potential Loss Facilities: Structural damage state probabilities and expected functionality for military facilities;</li> <li>- Direct Physical Damage – User-Defined Facilities</li> <li>- Direct Physical Damage – Advanced Engineering Building Model: Damage state probabilities; casualties; losses</li> <li>- Direct Physical Damage: For components of the 13 transportation and utility systems, damage state probabilities, cost of repair or replacement, and expected functionality for various times following earthquake by facility; For potable water, wastewater</li> </ul>		
--	--	--	---	---	--	--	--

						<p>and natural gas pipeline distribution systems, the estimated number of leaks and breaks; For potable water and electric power systems: estimate of service outages at Day 1, 3, 7, 30 and 90.</p> <ul style="list-style-type: none"> <li>- Induced Physical Damage             <ul style="list-style-type: none"> <li>- Inundated Areas,</li> <li>Fire Following Earthquake and Debris.</li> </ul> </li> <li>- Social Losses:             <ul style="list-style-type: none"> <li>Number of displaced households per census tract;</li> <li>Number of people requiring temporary shelter per census tract. Casualties per census tract in four categories of severity based on three different times of day (2 am, 2 pm and 5 pm).</li> </ul> </li> </ul> <p>Aggregate estimates of casualties by time of day, injury severity,</p>	
--	--	--	--	--	--	---	--

						and general occupancy class.		
<b>MAEviz</b>	MAE Center through the Earthquake Engineering Research Centers Program of the National Science Foundation under NSF Award No. EEC-9701785.	Open source platform: Eclipse RCP Program language: JAVA	It implements Consequence-Based Risk Management (CRM) to estimate the damage and the losses for buildings, bridges and lifeline (gas, water, electric facilities). For buildings, it estimates structural and nonstructural damage, economic losses and liquefaction damage. For bridges, it computes damage, loss of functionality and repair cost analysis. For lifelines it calculates the network damage and the repair rate analysis. Finally, it computes socio-economic losses such as shelter needs, fiscal and business interruption.  The hazard used when evaluating these fragilities is obtained by performing a transformation from elastic spectral	MAEviz can take into account liquefaction hazard in addition to ground shaking. The hazard response is spectral based and local site effects are taken into account. There are some default scenarios and probabilistic hazard maps in the catalog box however the user can upload their own hazard following a graphical interface. The user can also create the scenario using an	The MAEviz tool provides as default some inventories stored in tables and shapefiles. The inventory buildings contain information about the construction type, number of storeys, occupancy level, year of construction and building area. The user can upload their own inventory in the 'catalog box' and also can upload data about bridges and lifelines. The vulnerability functions were derived by structural analysis which considering the aleatory structural features	Output table, maps of economics losses, social losses, fiscal impact. Detailed or summary report for structural damage	Mid-America	<a href="http://mae.ceei.illinois.edu/software/software_maeviz.html">http://mae.ceei.illinois.edu/software/software_maeviz.html</a>

			<p>acceleration to elastic spectral displacement without regard for inelasticity in building response.</p> <p>Based on analyzes for structural damage and optional nonstructural damage, MAEViz compute the direct economic losses. More additional economic and socioeconomic analyses are available: the building repair cost based on the structural damage and building type, the building retrofit cost estimation, the number of casualties and the fiscal impact.</p>	<p>analysis. The user has to provide the spectrum type, the earthquake location, the coordinates of the region of interest and some advanced parameters such as the fault type, the dip angle, etc.</p>	<p>uncertainty and the excitation uncertainty. The fragility curves have been developed for construction typical of the Mid America region and provide the conditional probability of being in, or exceeding a particular damage state given by the seismic demand parameter. Three fragility curves are provided and four damage states are obtained by difference between adjacent curves.</p>			
<b>OpenQuake</b>	Global Earthquake Model Foundation (GEM)	OpenSource. For GIS visualization is integrated with QGIS	Can be used for various types of analyses (providing logic tree support), combining input from the hazard module (or user provided), exposure and	Classical PSHA (hazard curves, hazard maps, uniform hazard spectra, disaggregation	Inputs for the damage assessment step consist in exposure models (i.e., GEM building taxonomy) in	- asset-specific loss exceedance curves, average annual loss, loss maps, building typology disaggregation - event loss tables, loss exceedance	Worldwide, with major contributions to Australia, Arabia, Canada,	<a href="https://www.globalquakemodel.org/openquake">https://www.globalquakemodel.org/openquake</a>

			<p>vulnerability input consisting mainly of fragility or vulnerability functions:</p> <ul style="list-style-type: none"> <li>- Scenario Damage Assessment</li> <li>- Scenario Risk Assessment</li> <li>- Classical Probabilistic Seismic Damage Analysis</li> <li>- Classical Probabilistic Seismic Risk Analysis</li> <li>- Stochastic Event Based Probabilistic Seismic Damage Analysis</li> <li>- Stochastic Event Based Probabilistic Seismic Risk Analysis</li> <li>- Retrofit Benefit-Cost Ratio Analysis</li> </ul>	<p>n), Event-based hazard (stochastic earthquake event sets and ground motion fields, hazard curves, hazard maps), Scenario hazard (single event - stochastically generated ground motion fields).</p> <p>5 typologies for modeling seismic sources, 100+ GMPEs implemented and tested.</p>	<p>terms of built areas or single assets. Fragility models are then applied in order to estimate damage distribution and consequence functions for loss estimation, or directly vulnerability functions.</p>	<p>curves - asset specific and aggregated, average annual loss, loss maps, loss disaggregation</p> <ul style="list-style-type: none"> <li>- loss statistics, loss maps</li> <li>- collapse maps, damage distribution per asset and building typology</li> </ul>	<p>Caribbean and Central America, Europe, Indonesia, South America, Southeast Asia, Taiwan and South Africa but also Global Hazard and Risk Earthquake Models.</p>	
<b>PAGER</b>	USGS (United States Geological Survey)	Open source	<p>Loss estimates are only based on empirical models (linking intensity with casualty probability) while other estimates such as the distribution of impacted</p>	<p>Updated ground-motions maps are provided by the USGS ShakeMap® system</p>		<p>The number of people exposed to various levels of shaking is then calculated by combining the maps of predicted ground shaking with Oak Ridge National</p>	<p>World-wide</p>	<p><a href="https://earthquake.usgs.gov/data/pager">https://earthquake.usgs.gov/data/pager</a></p>

			<p>buildings make use of the other methods.</p> <p>PAGER generates estimates of the ranges of potential fatalities and economic losses based on country-specific loss models that account for differences in construction practices and building vulnerabilities around the globe. In addition, the PAGER system estimates potential for earthquake-induced landslides.</p>			<p>Laboratory's Landscan global population database.</p> <p>Pager report contain:</p> <ul style="list-style-type: none"> <li>• Summary of the basic earthquake parameters;</li> <li>• Impact scale alert level for fatalities and economic losses</li> <li>• Table showing population exposed to different MMI levels</li> <li>• Map of MMI contours</li> <li>• Region specific structures and general description of vulnerability of the buildings in the region</li> </ul>		
<b>QLARM</b>	ICES Foundation		<p>Parameters introduced in the QLARM database are the following: 1) soil amplification factors; 2) distributions of building stock and population into vulnerability classes; and 3) the most recent</p>	<p>Approaches to estimate soil amplification: (a) local approach based on the existing data regarding soil properties,</p>	<p>Vulnerability classes are assigned to different building types considering the vulnerability table given by the European</p>	<p>QLARM provides estimates on the number of fatalities and average damage on buildings on global scale.</p> <p>It is used daily: a) in real-time to</p>	World-wide	<p><a href="http://www.icesfoundation.org/Pages/CustomPage.aspx?ID=122">http://www.icesfoundation.org/Pages/CustomPage.aspx?ID=122</a>; Trendafilosky et al (2009)</p>

			<p>population numbers by settlement or district.</p> <p>The building and population distributions are constructed using the percentage of the number of buildings and population belonging to a particular vulnerability class. The building damage in QLARM is calculated using the European Macroseismic Method (Giovinazzi, 2005). The human losses are estimated using the casualty event-tree model proposed by Stojanovski and Dong (1994). Simplified daily population dynamics as suggested by Coburn and Spence (2002) are integrated.</p>	<p>microzonation, and geological maps to derive the amplification factor for each discrete city model; (b) global approach based on Vs30 values derived from topographic slopes</p>	<p>Macroseismic Scale EMS-98.</p>	<p>distribute alert messages in case of large earthquake worldwide daily and b) in scenario mode to estimates losses to be expected in future events in high-risk seismic zones of the globe.</p>		
<b>SEISMOCA RE</b>		No	<p>It is a GIS tool for scenario-type investigations of seismic risk of existing cities</p>	<p>Based on deterministic analysis and PGA values, accounting also for soil amplification</p>	<p>Damage computation is empirical. Exposure can consist of buildings,</p>	<p>Building damage. Casualties. Cost of damage</p>	Greece	<p>Anagnostopoulos et al. (2008)</p>

				factors provided by the users	infrastructures and population.			
<b>SELENA</b>	NORSA R, Universidad de Alicante	Open-source (Matlab or others)	SELENA is an adaptation of the HAZUS-MH Methodology, but with additions such as integration of other demand spectrums (EC8, Indian IS 1983 and Cuba NC 46-2013, beside IBC 2006).  CSM, MADRS or IDCM methods are used for determining the building performance points. A logic tree approach is used.	Has modules for probabilistic, deterministic or Real-time input analysis.  The user has to supply (depending on chosen method) earthquake sources, (empirical) GMPEs (some included), soil maps and corresponding ground-motion amplification factors. It can account for topographic amplification of ground motion (ICMS 2008 Italy and	The user has to supply built area or number of buildings in different model building types, capacity curves and fragility curves corresponding to each of the model building types and finally cost models for building repair or replacement.	SELENA will compute the probability of damage in each one of the four damage states (slight, moderate, extensive, and complete) for the given building types, fatalities, people in need of shelter, reconstruction costs, the amount of debris, the total number of uninhabitable buildings and displaced households.  Outputs are supplied as text files or maps, using the RISE additional software (which provides .kml output for Google Earth).	Norway, Romania, Haiti, India, Cuba	<a href="https://personal.ua.es/en/sergio-molina/selena-rise-en.html">https://personal.ua.es/en/sergio-molina/selena-rise-en.html</a>

				EC8 methods included).				
<b>SISMOTO OL</b>	Junta de Andalucía, Universidad de Almería, Universidad de Alicante	OpenSource. For GIS visualization is integrated with ESRI ArcGis	Provides Empirical and Analytical damage computation	Deterministic or Pre-computed ShakeMap, relies on Spectral Acceleration. Can account for site effects, based on soil and topographic amplification factors.	Buildings and population. Can account for soil-structure interaction, using an empirical method	Shakemaps in terms of intensity and spectral acceleration. Building and dwelling Damages. Economic losses. Casualties and Shelter	Spain	Lopez Hidalgo et al. (2022)

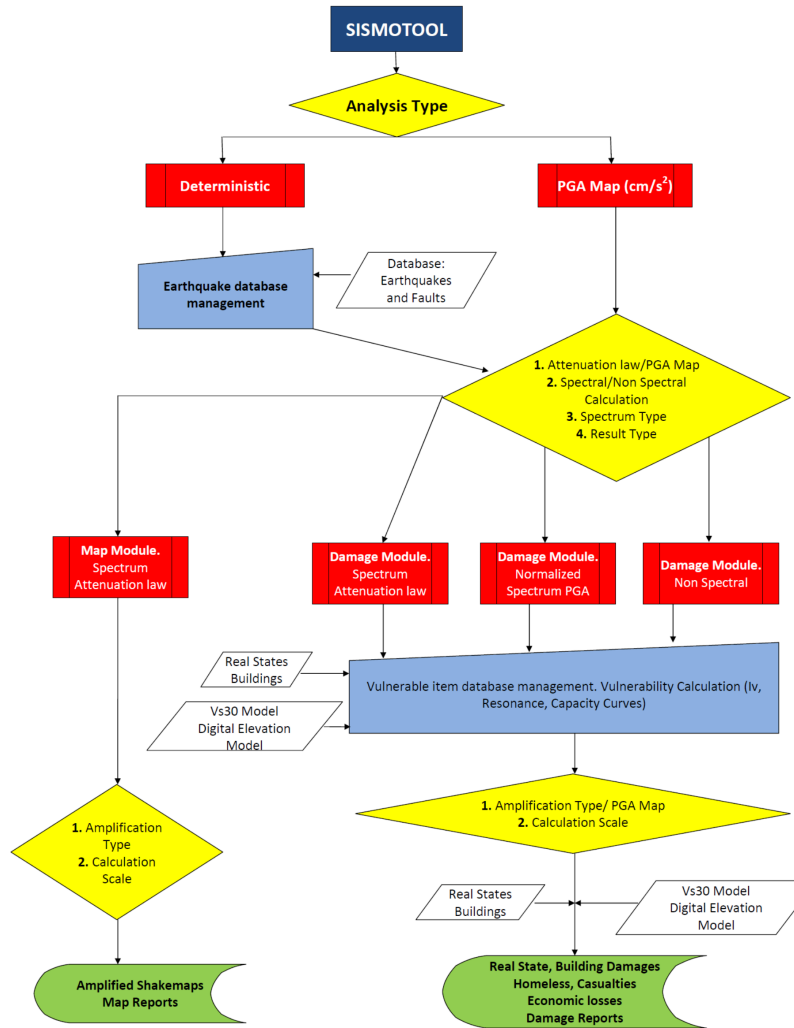


Figure 14 Flowchart of SISMOTOOL (Lopez Hidalgo et al., 2022)

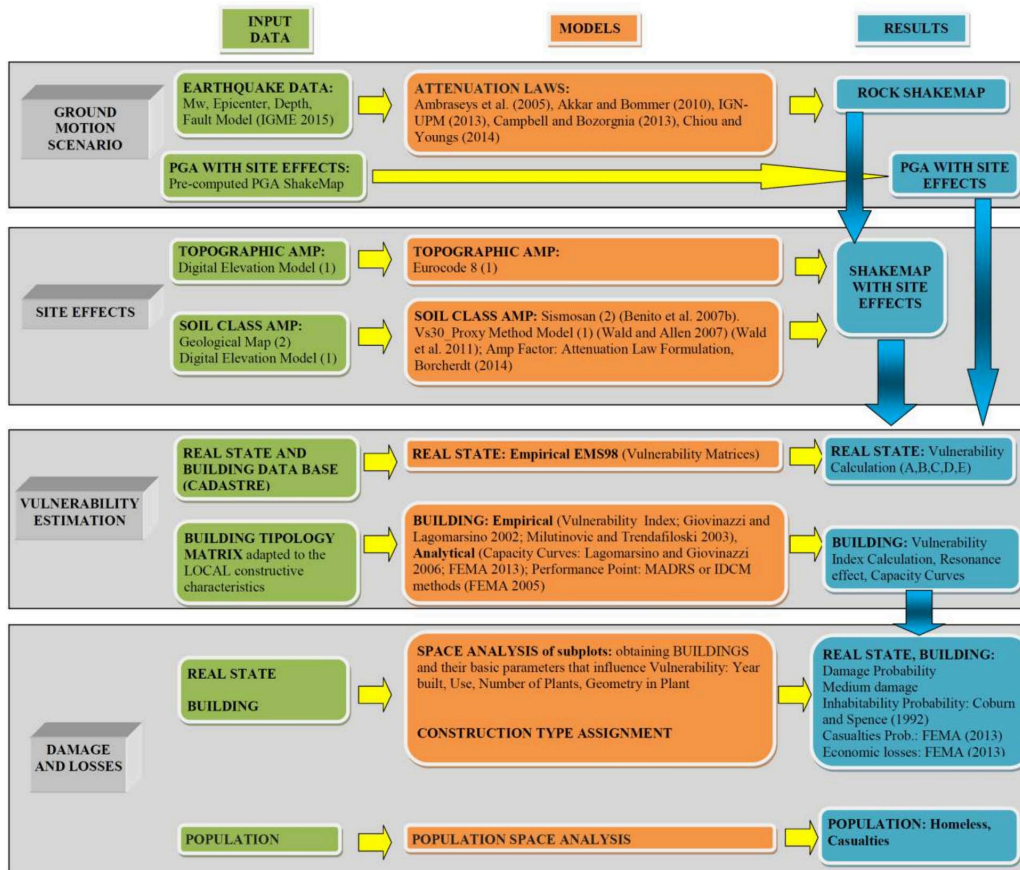


Figure 15 SISMOTOOL development and computation scheme (Lopez Hidalgo et al., 2022)

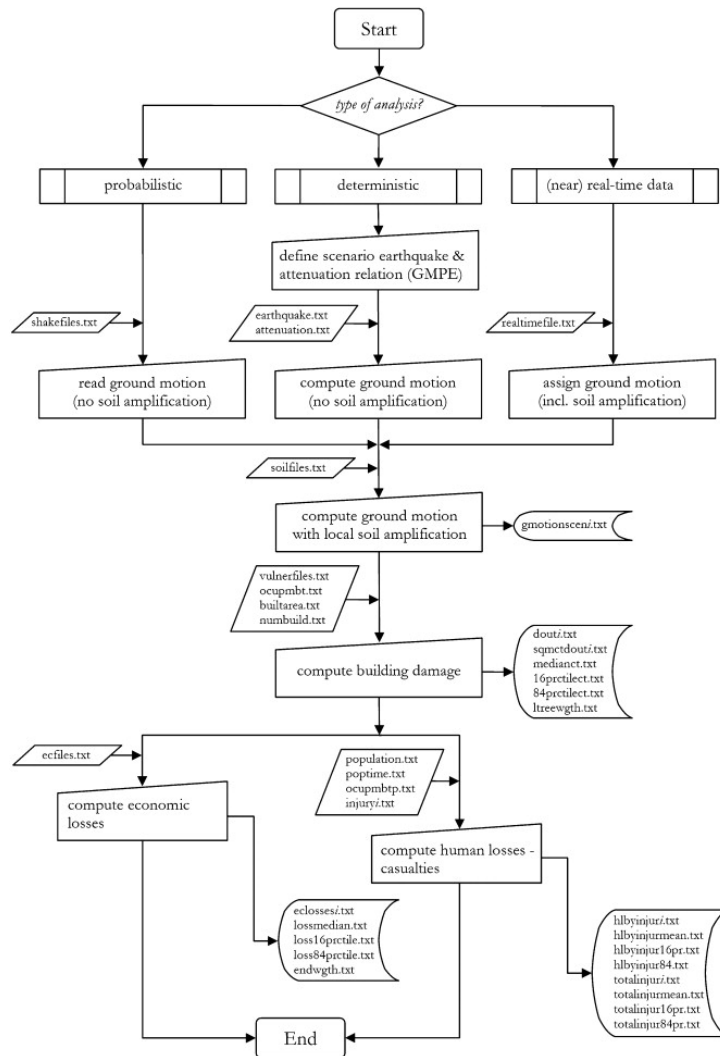


Figure 16 SELENA computational flowchart (from Molina et al., 2010)

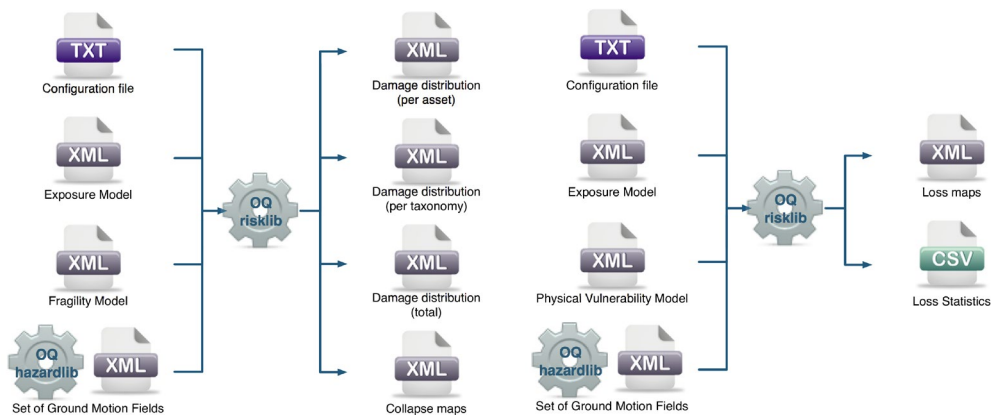


Figure 17 OpenQuake Scenario Damage (left) and Risk (right) Calculator input/output structure (GEM, 2024)

## 3. Concept for the Multicare RSLE

### Envisioned methodology

Based on the literature review and considering MULTICARE objectives, we propose the use of the following approach (Figure 18) for an RSLE in the MULTICARE case-study areas in Romania - Tecuci (at city level) and Bucharest (at individual building level):

- **Use input ground motion parameters from the Romanian Seismic Network of INFP and accelerometers installed within the MULTICARE Project.** This can consist of ground motion values from the stations (PGA, SA at relevant periods for the analyzed structural typologies, PGV, PGD and others if needed – depending on the definition for fragility and vulnerability functions), earthquake parameters (magnitude, depth, latitude, longitude, focal mechanism parameters) sent by the operational Earthquake Early Warning System (Marmureanu et al., 2021) and by other automated and manual systems. INFP also collects “Did you feel it?” data through two types of questionnaires; this information can be also of great use for refining intensity maps and applying empirical equations to estimate casualty intervals. This would rely on the USGS Pager level 0 method, which was also implemented by INFP within version 3 of the SeisDaRo system (Toma-Danila et al., 2021; 2017). As the Romanian Seismic Network of INFP is part of the EIDA initiative (a distributed federation of datacenters established to securely archive seismic waveform data and metadata gathered by European research infrastructures; <https://www.orfeus-eu.org/data/eida/>), the RSLE will be easily applied at different scales and areas.
- **For individual building assessment, structure-specific intensity measures will be computed, based on the recorded free-field data,** leveraging on known characteristics like the fundamental period of the structure. In operational conditions and for post-earthquake assessment, fragility functions combined with actual intensity measures (PGA, PGV, spectral ordinates) will enable us to estimate the probability of reaching or exceeding a certain damage state.
- Another approach to make use of actual recorded strong motion data is to compare, if available, the design spectrum of a specific building with the free-field response spectrum of the earthquake and check for any exceedances, at specific periods (Balan et al., 2019, Dominguez Reyes et al., 2017, Su et al., 2006, Malcioglu et al., 2022).
- For buildings with extensive instrumentation (at multiple floors), **the rapid computed inter-story drift can be used as a proxy of the damage state,** according to international or national limit state displacement thresholds (Hazus, P100-1/2013 Romanian Seismic Design Code etc.). In addition, the changes in dynamic characteristics (pre- and post-earthquake) can also be an indicator of damage occurrence within structural elements. This will be further explored within MULTICARE WP9 tasks.
- Customize already available open-source solutions that proved to be successful. As such, **for obtaining relevant intensity measures we plan to rely on the ShakeMap 4 system and approach.** The Romanian case-study areas have particularities when it comes to the type of earthquake sources that can affect them. Tecuci can be affected both by intermediate-depth earthquakes in the Vrancea Area, as well as crustal earthquakes in the vicinity. Bucharest can be affected by intermediate-depth earthquakes in the Vrancea Area, but considering local site effects is needed, as reflected by previous major earthquakes in 1977, 1986 or 1990. Therefore, integration of specific Ground Motion Models is necessary. This was previously started (Marmureanu et al., 2021), but it needs to be continued and improved. It is

worth mentioning that nowadays ShakeMap uses GMMs from the OpenQuake library and shares Python scripts.

- The 2020 European Seismic Hazard and Risk Models (Crowley et al., 2021a; Danciu et al., 2021) are among the proof that OpenQuake is a mature software capable of delivering products relevant for risk analysts and policymakers. Given that the INFP is already familiar with the software and the way hazard, exposure and vulnerability models can be integrated (having worked within the SERA Project to define parts of the European model for Romania), it seems a good choice also for MULTICARE. **Using OpenQuake as engine for RSLE** is feasible and the fact that the code is open-source will make it easy to add new features as well as connectivity to other MULTICARE tools such as the decision-support platform developed within WP7. As new features we will be able to test new resilience functions and functions regarding non-structural and multi-risk components to be developed within MULTICARE, as well as fragility and vulnerability functions using non-classical intensity measures such as interstory drift or Arias Intensity, depending also on the outcomes of individual building modelling and monitoring. Also, OpenQuake already has a module which allows the computation of liquefaction potential, because of an earthquake scenario – which is of interest for the MULTICARE objectives. Compared to other types of earthquake-triggered hazards, liquefaction is most representative of our case-study areas.
- Special focus will be given to the way results are presented and evaluated; **disaggregation of the damage results**, per building typology, will be able to reflect limitations in the selection of fragility functions in accordance also with ground motion recordings and estimates, but also highlight damage patterns throughout a city such as Tecuci. Making sure that **output is in GIS format** (not just .csv but also .geojson or .shapefile, for proper representation of polygons) will enable a useful spatial representation. Standardized data formats will also ensure compatibility (through for example API protocols) with the MULTICARE decision-support platform.

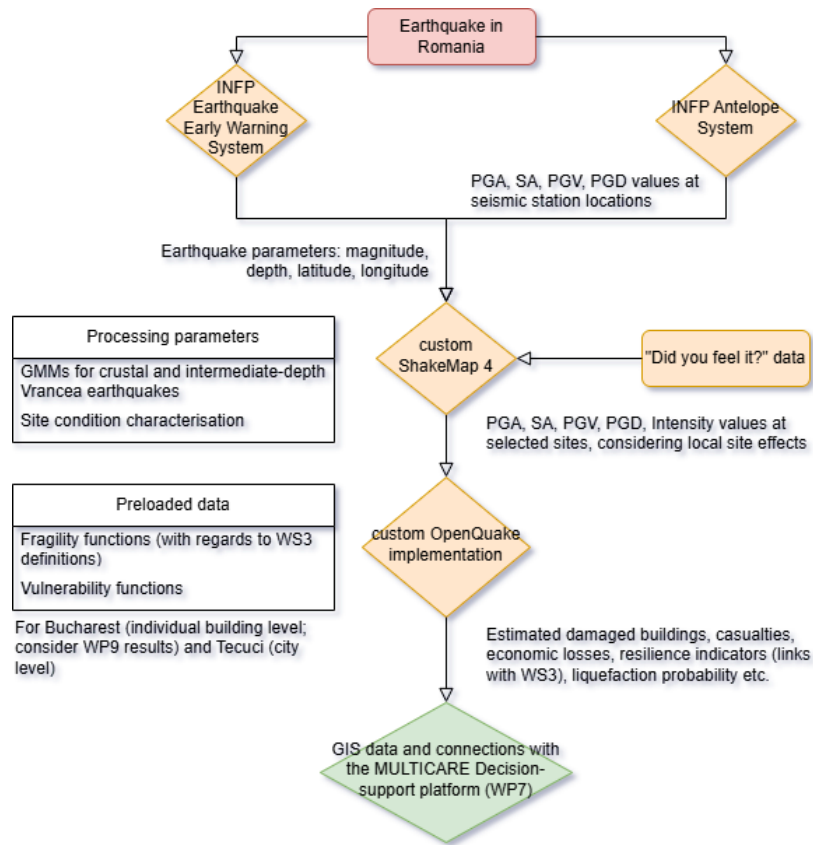


Figure 18 Proposed framework for the MULTICARE RSLE system

## Preliminary testing

To show the potential of the proposed methodology for the MULTICARE RSLE system, we started testing the OpenQuake developer (devel) version (3.22), which allows changes in the code (GEM, 2024).

One of the first challenges was that only one GMPE developed specifically for intermediate-depth Vrancea earthquakes in Romania is included by default in OpenQuake: Manea et al. (2022). To facilitate a hazard estimate based on multiple GMMs, we integrated two other GMPEs developed specifically for the Vrancea area: Sokolov et al. (2008) and Vacareanu et al. (2015). The results of running the three GMPEs can be seen in Figure 19. These were obtained not only for maximum ground acceleration values (PGA), but also for spectral accelerations at periods defined by the fragility functions available for the buildings ( $S_a$  at 0.3, 0.6, 0.7 and 1.0 seconds). To run earthquake scenarios for intermediate-depth Vrancea earthquakes and crustal earthquakes, a grid consisting of 3313 points was used as an input file in OpenQuake, with a longitude spacing of 7.77 km and a latitude spacing of 11.11 km between them, which covered the entire territory of Romania. Each point had representative values for  $V_{s30}$  and  $f_0$ . This file was provided by Manea et al., and is based on previous articles including: Manea et al. (2016, 2019, 2020, 2021b) and Coman et al. (2020). Additionally, characteristics about belonging to a specific region (back-arc, fore-arc, along-arc or Vrancea, Focsani, Nord, Est etc.) were added, depending on the zonation provided by each GMM.

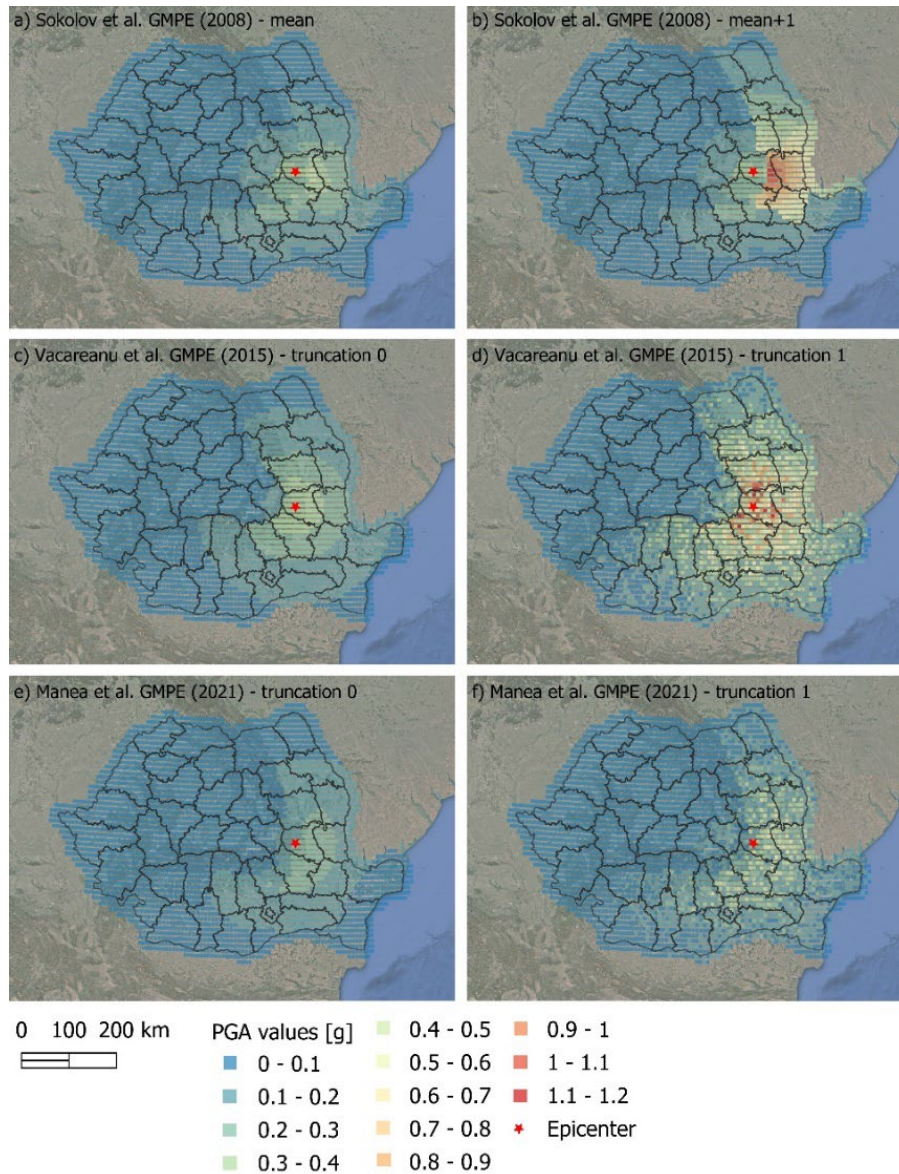


Figure 19 Ground motion distribution map (in PGA), for a scenario of the March 4, 1977 Vrancea earthquake ( $M_w$  7.7, 94 km depth), using 3 ground motion prediction equations (GMPE): a) and b) Sokolov et al. (2008), c) and d) Vacareanu et al. (2015), e) and f) Manea et al. (2022), and untruncated and truncated forms with coefficient 1 of the equations

For crustal earthquakes, OpenQuake has a very large number of GMMs that can be used: more than 150, some with multiple additional forms. Considering the recent results of testing equations for crustal earthquakes in Romania (Theodoulidis et al., 2024), 4 GMMs were chosen for the earthquake scenario in the Tecuci area: Boore et al. (2014), Cauzzi et al. (2014), Chiou and Youngs (2014) and Kale et al (2015; the version for Iran). OpenQuake also allows the application of weights regarding the contribution of these equations to the result, but equal weights have been used for testing for now. The results obtained can be viewed in Figure 20 and Figure 21.

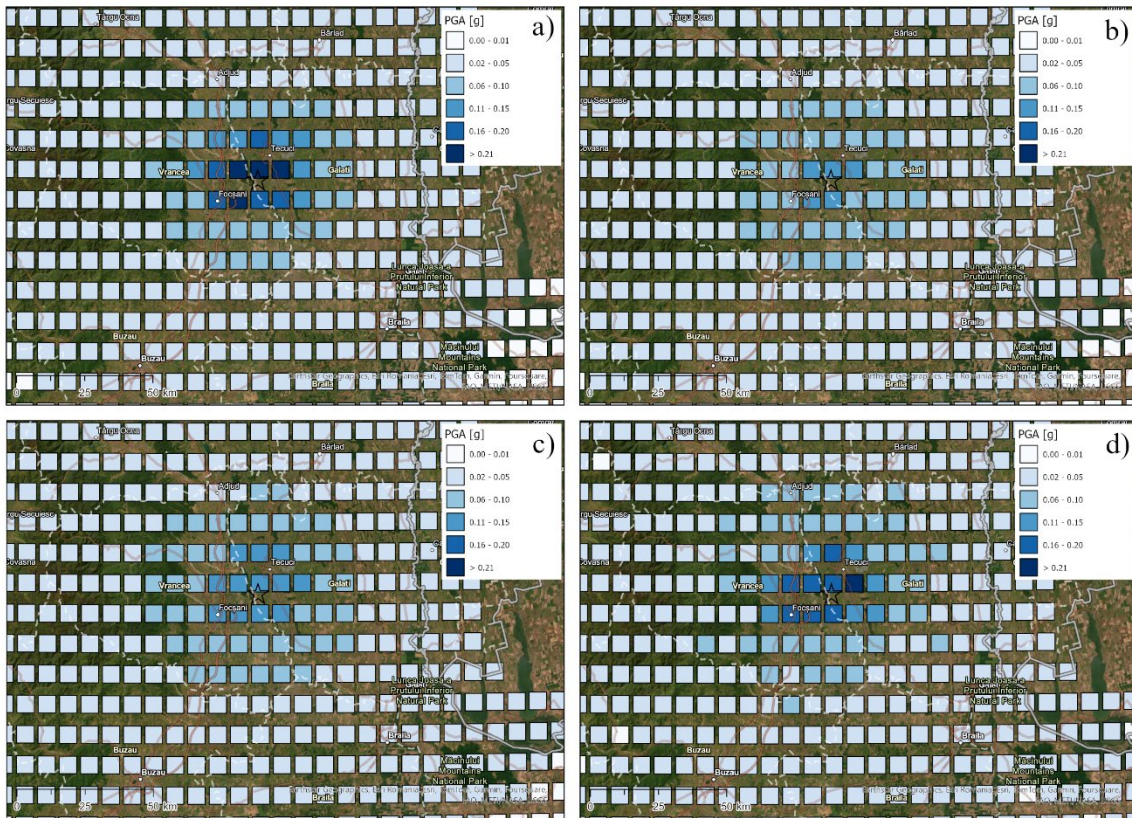


Figure 20 Ground motion distribution map (in PGA values), for a crustal earthquake scenario in the Tecuci area (Mw 6.0, 20 km depth), obtained for the untruncated form of 4 GMPEs: a) Boore et al. (2014), b) Cauzzi et al. (2014), c) Chiou and Youngs (2014) and d) Kale et al. (2015; Iran)

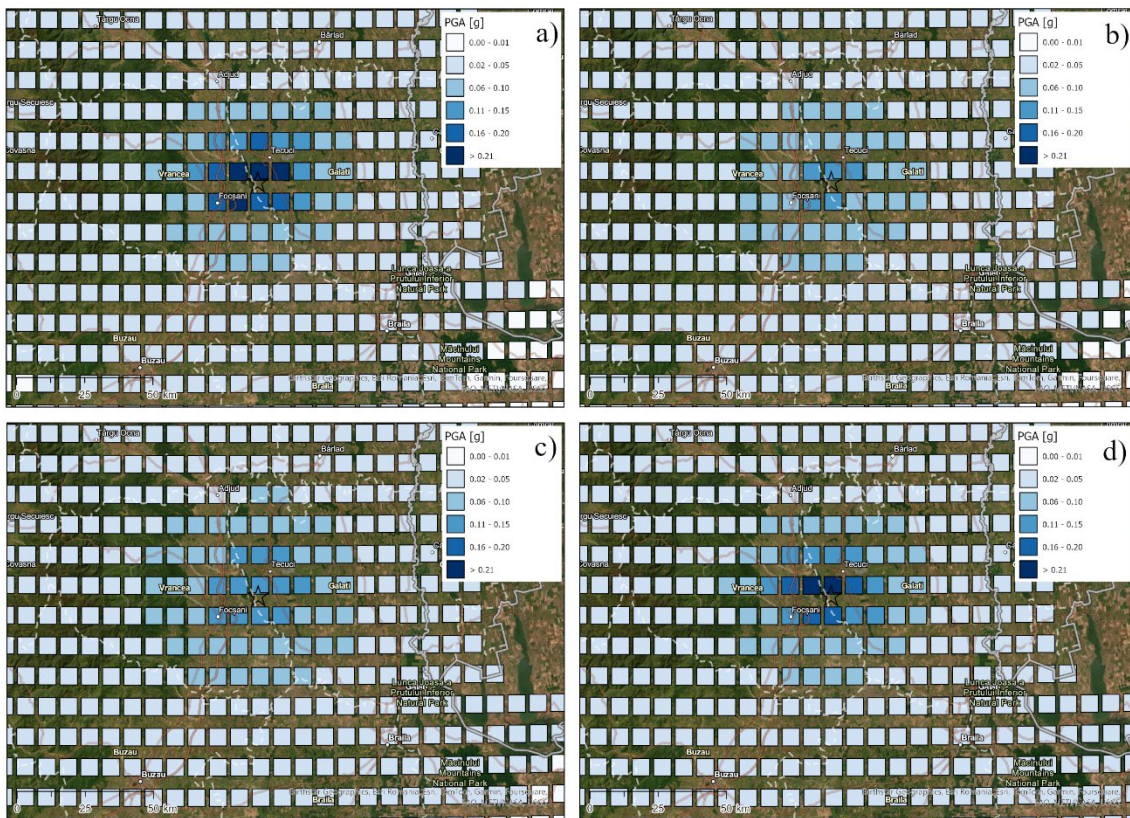


Figure 21 Ground motion distribution map (in PGA values), for a crustal earthquake scenario in the Tecuci area (Mw 6.0, 20 km depth), obtained for the truncated 1 form of 4 GMPEs: a) Boore et al. (2014), b) Cauzzi et al. (2014), c) Chiou and Youngs (2014) and d) Kale et al. (2015; Iran)

Figures highlight that the results we currently obtain through OpenQuake are representative of the characteristics of earthquakes in Romania, and the premises for successfully running the implemented codes as well as the input files for seismic hazard are very good, for a near real-time implementation. As expected, there is a large variability of the acceleration values, for different shapes of the GMMs, but the prior use of a ShakeMap-type methodology, which also considers real earthquake recordings, will provide values closer to reality. Another important aspect to mention is the fact that starting with version 4 of ShakeMap, it directly uses the OpenQuake GMPE library, which allows us to use the GMMs for Vrancea there as well, facilitating interoperability between systems.

Regarding the exposure and vulnerability database, a first step was to use data from the European Seismic Risk Model 2020, to which the INFP team contributed, for Romania. It contains data from the 2011 Census at the UAT level, additionally processed to refine the distribution by building typology, respecting the specifications of the SERA Project and the Global Earthquake Model taxonomy, as well as the fragility functions (of two types: ShakeMap and Various), proposed for the European Model. Here are some features of this model:

- Exposure data on residential, industrial, and commercial buildings (although the last two categories have significant limitations, being derived from county-level data);
- 243 building typologies with different fragility functions; these refer to both structural system, construction period and height regime;
- Fragility or vulnerability functions for reconstruction costs due to structural damage and for the possibility of loss of life for a diurnal, nocturnal or transit scenario.

Functions are defined in terms of both PGA and SA, depending on representativeness.

More details about this model can be found in Crowley et al. (2020, 2021b). By validating the functionality of this already certified model, we believe that we have a solid starting point for implementing a model even more appropriate to the specifics of Romanian construction and population distribution.

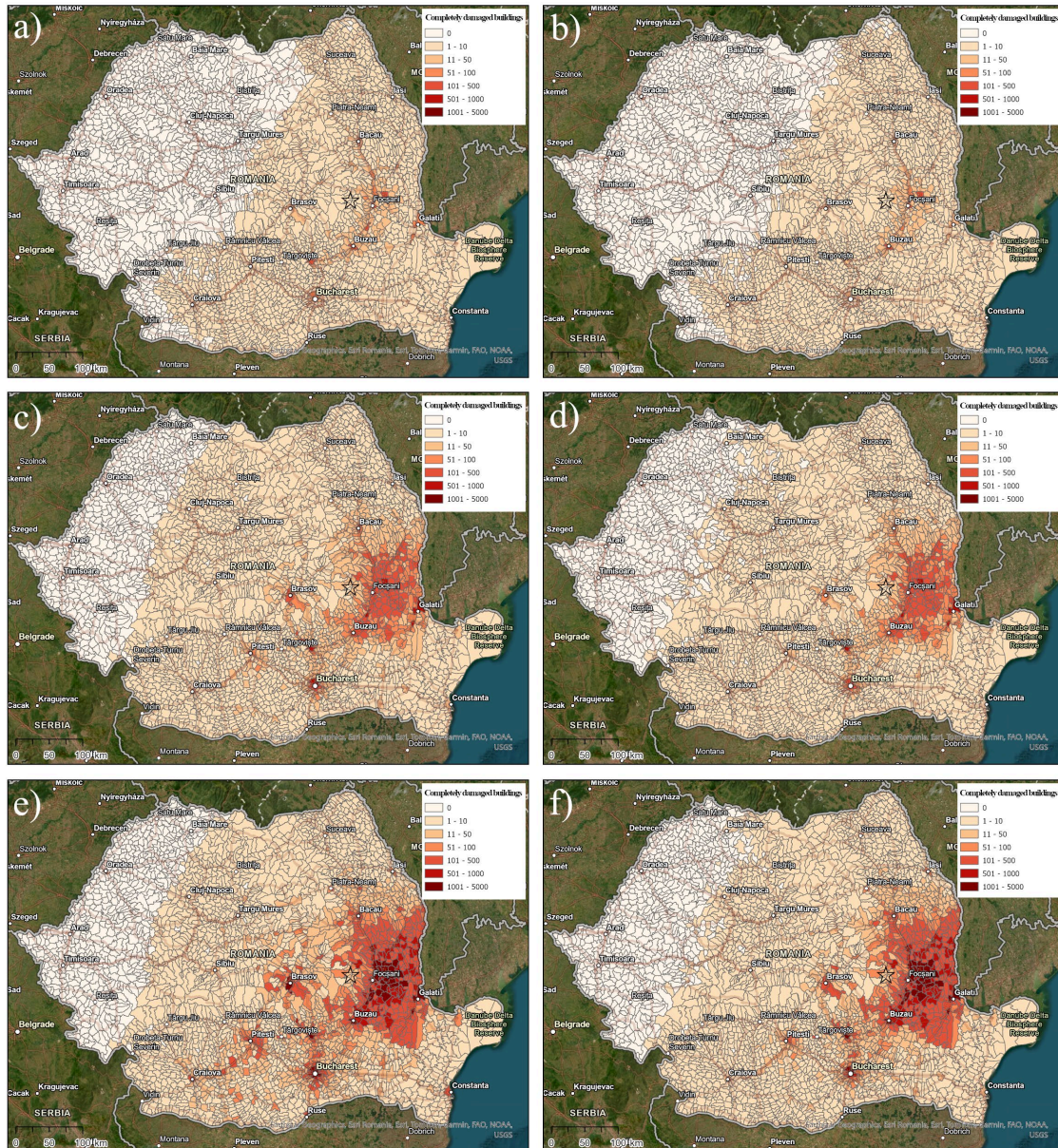


Figure 22 Estimates of the number of completely damaged residential buildings, obtained for scenarios of the March 4, 1977 Vrancea earthquake ( $M_w$  7.7, 94 km depth; with truncation levels 0 and 1); the minimum (top), median (middle) and maximum (bottom) values are shown, obtained with the ESRM20 fragility function set for ShakeMap (a, c and e) and Various (b, d and f)

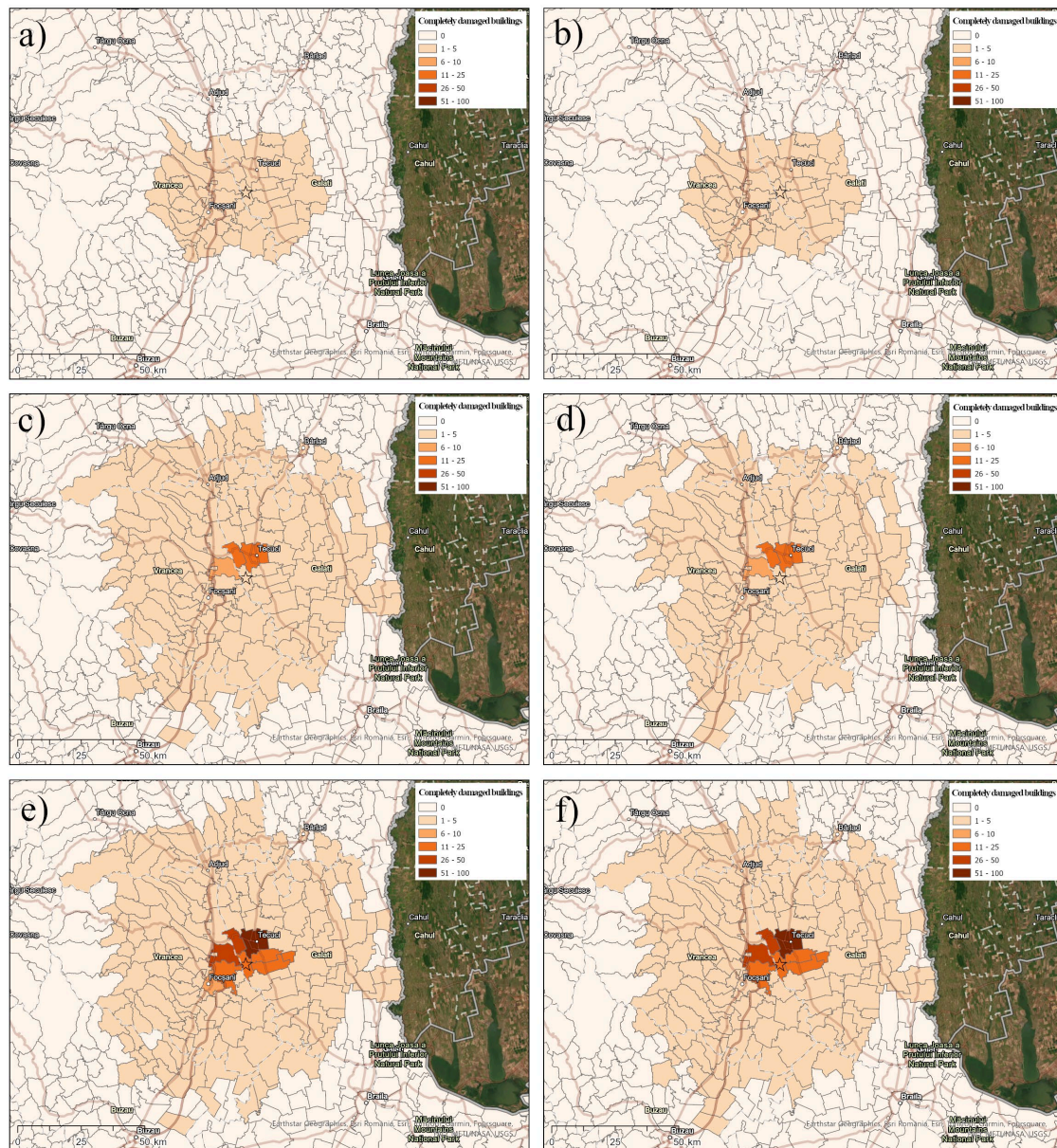


Figure 23 Estimates of the number of completely damaged residential buildings, obtained for crustal earthquake scenarios in the Tecuci area ( $M_w$  6.0, 20 km depth; with truncation levels 0 and 1); the minimum (top), median (middle) and maximum (bottom) values are shown, obtained with the ESRM20 fragility function set for ShakeMap (a, c and e) and Various (b, d and f)

To calculate the number of victims or direct economic damage, based on the estimates of the number of damaged buildings, vulnerability functions can be used directly. The European Seismic Risk Model also contains such vulnerability functions for the same structural typologies in the fragility functions, so we tested them to see results for estimated number of severely injured or deceased persons.

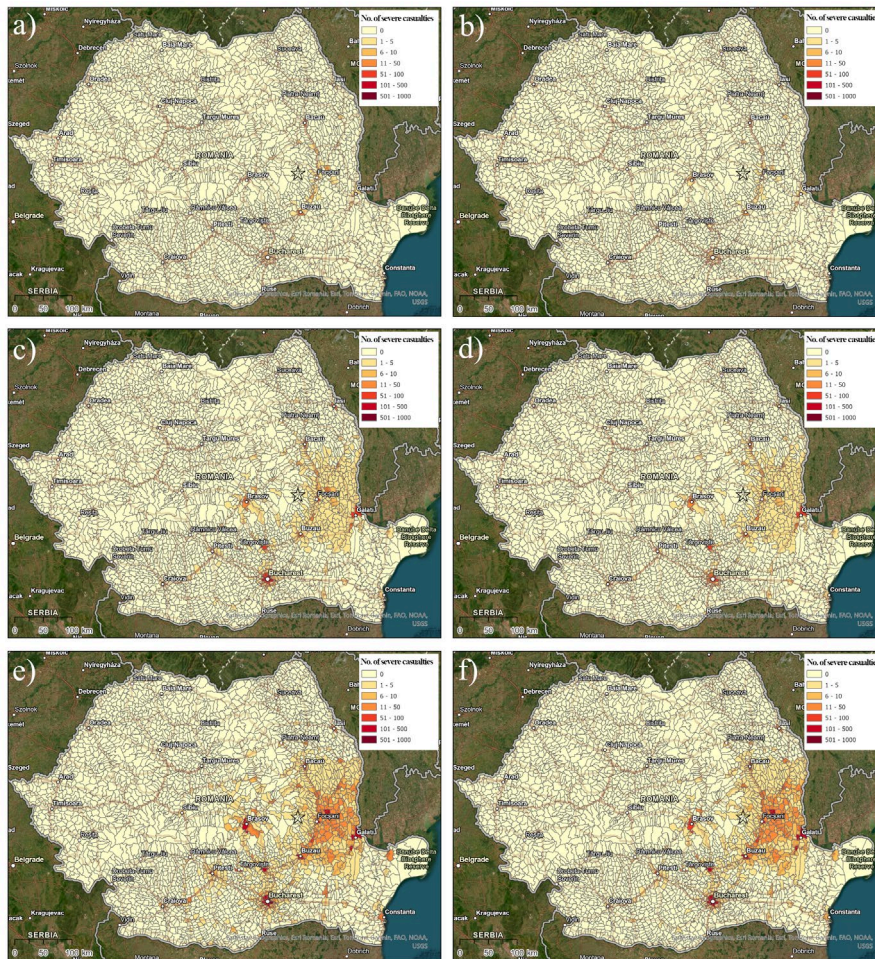


Figure 24 Estimates of the number of persons severely injured or deceased, obtained for a scenario of the earthquake of March 4, 1977 (Mw 7.7, 94 km depth); the minimum (top), median (middle) and maximum (bottom) values are presented, obtained with the set of vulnerability functions from ESRM20 for ShakeMap (a, c and e) and Various (b, d and f)

The tests show general results for the Bucharest and Tecuci areas. Our plan for now was just to prove the functionality of OpenQuake – as a solution to build our RSLE upon and embed new data and methods. The next step will be to provide an RSLE at the city level, accounting in greater detail for local site conditions (use a denser grid in ShakeMap or an estimation of ground motion parameters directly at selected sites) and exposure and vulnerability data.

### 3. Conclusion

There are multiple methods and open-source software for rapid seismic loss estimation that can be used and improved within the MULTICARE Project. The traditional approach based on fragility, consequence or vulnerability functions for building typologies and their assets is one that is still preferable. However, extending this approach by integrating additional ground motion parameters (not just PGA), accounting for degradation over time, and incorporating interventions to buildings (such as modelling the behavior of the building in Bucharest to be retrofitted within the MULTICARE Project), might result in improved loss estimates. As practice showed, the available methods can be sufficient to express damage and loss, but limitations many times came from the data that is being

used for computation: local site condition description, GMM selection, exposure and vulnerability datasets, as well as data resolution. By focusing in MULTICARE on two specific case-study areas (Bucharest and Tecuci, in Romania) we will be able to show through our RSLE how much higher quality data can influence the results of more generic datasets. The fact that case-study areas can be affected by different types of earthquakes (both intermediate-depth and crustal) will be a point of interest in showing, in a disaggregated way, differences in terms of impact. By trying to incorporate multi-hazard and multi-risk dimensions in the RSLE, we will provide more relevant outputs for the MULTICARE Decision-support system that will help stakeholders to understand the bigger picture in case of major earthquakes.

## Annex 1. List of countries that have implemented ShakeMap

Name	Location	Institution(s)	Method	Status	References
<b>Outside Europe</b>					
USGS ShakeMap®	U.S./Worldwide	USGS NEIC	v3.5: Weighted interpolation v4: conditional MVN	Operational	<a href="http://earthquake.usgs.gov/data/shakemap">earthquake.usgs.gov/data/shakemap</a> Wald et al., 1999; Wald et al., 2005;
BMKG shake-map	Indonesia	BMKG	ShakeMap® v3.5	Operational	<a href="http://inatews.bmkg.go.id/">http://inatews.bmkg.go.id/</a> Pramono et al., 2017
GA ShakeMap and DYFI	Australia	Geosciences Australia	ShakeMap® v4 DYFI v4	Operational	<a href="https://earthquakes.ga.gov.au/">https://earthquakes.ga.gov.au/</a> Allen et al., 2019
BCSIMS ShakeMap	British Columbia	British Columbia Smart Infrastructure Monitoring System	Custom code based on ShakeMap® v3.5	Operational	<a href="http://www.bcsims.ca/">http://www.bcsims.ca/</a>
KMA ShakeMap	South Korea	Korea Meteorological Agency	ShakeMap® v4, customized	Operational	<a href="http://www.weather.go.kr/XML/INTERNET/INT3_20190419111643.html">http://www.weather.go.kr/XML/INTERNET/INT3_20190419111643.html</a>
UAE ShakeMap	Dubai	Dubai Municipality	ShakeMap® v3.5	Operational	<a href="https://shakemap.dm.ae/shake/">https://shakemap.dm.ae/shake/</a> Al Khatibi et al., 2014
<b>In Europe</b>					

Name	Location	Institution(s)	Method	Status	References
ShakeMap apEU	Euro-Mediterranean area	EMSC, ETH, ORFEUS, EFEHR	ShakeMap@ v4	Operational	<a href="https://shakemap.eu.ingv.it/">https://shakemap.eu.ingv.it/</a> Cauzzi et al., 2018
SED shake-map	Switzerland	ETH SED	ShakeMap@ v3.5	Operational	<a href="http://www.seismo.ethz.ch/en/home/">http://www.seismo.ethz.ch/en/home/</a> Cauzzi et al., 2014
IPMA shake-map	Portugal	IPMA	ShakeMap@ v3.5	Operational	<a href="http://shakemap.ipma.pt/">http://shakemap.ipma.pt/</a> Marreiros et al., 2012
INFP shake-map	Romania	INFP, NIEP	ShakeMap@ v3.5 ShakeMap@ v4	Operational Under implementation	<a href="atlas2.infp.ro/~shake/shakemap">atlas2.infp.ro/~shake/shakemap</a>
SisPyr	Pyrenees (France, Spain)	ICGC, OMP, BRGM, IGN, UPC	ShakeMap@ v3.5	Operational	<a href="http://www.sispyr.eu/shakemap/">http://www.sispyr.eu/shakemap/</a> Bertil et al., 2012
POCRISC shake-map	Pyrenees (France, Spain)	ICGC, BRGM	ShakeMap@ v4	Under implementation (beta version online)	<a href="https://sismocat.icgc.cat/shakemap/index.php?lang=en">https://sismocat.icgc.cat/shakemap/index.php?lang=en</a>
BCSF shake-map	France (including West Indies overseas territories)	BCSF	ShakeMap@ v3.5	Operational	<a href="http://www.franceseisme.fr">www.franceseisme.fr</a> Schlupp, 2016
BCSF shake-map	France	BCSF	ShakeMap@ v4	Under implementation	Schlupp et al., 2019
CASSAT	South-East France	GeoAzur	ShakeMap@ v3.5	Operational	<a href="http://sismoazur.oca.eu/">http://sismoazur.oca.eu/</a>
RISVAL-FR	South-East France	GeoAzur	ShakeMap@ v4	Under implementation	Bosco et al., 2019
IMO shake-map	Iceland	Icelandic Meteorological Office	ShakeMap@ v3.2	No longer maintained	<a href="http://hraun.vedur.is/ja/alert/shake">hraun.vedur.is/ja/alert/shake</a>
NOA shake-map	Greece	NOA	ShakeMap@ v3.5	Operational	<a href="http://accelnet.gein.noa.gr/shakemaps">accelnet.gein.noa.gr/shakemaps</a>

Name	Location	Institution(s)	Method	Status	References
EPPO-ITSAK shake-map	Greece	EPPO-ITSAK	ShakeMap@ v3.5	Operational	<a href="http://shakemaps.itsak.gr">shakemaps.itsak.gr</a>
INGV shake-map	Italy	INGV	ShakeMap@ v3.5	Operational	<a href="http://shakemap.rm.ingv.it">shakemap.rm.ingv.it</a> Michelini et al., 2008
RSNI shake-map	North-West Italy	RSNI	ShakeMap@ v3.5	Operational	<a href="http://www.distav.unige.it/rsni/seismicity.php?lang=en">http://www.distav.unige.it/rsni/seismicity.php?lang=en</a>
RISVAL-IT	North-West Italy	ARPA-Piemonte	ShakeMap@ v4	Under implementation	Bosco et al., 2019
KNMI shake-map	Groningen (Netherlands)	KNMI	ShakeMap@ v3.5	Operational	<a href="http://www.knmi.nl/nederland-nu/seismologie/aardbevingen">www.knmi.nl/nederland-nu/seismologie/aardbevingen</a>

\* this table is modified after Guerin-Marthe et al. (2021)

## References

- Allen, T. I., & Wald, D. J. (2009). On the use of high-resolution topographic data as a proxy for seismic site conditions (VS 30). *Bulletin of the Seismological Society of America*, 99(2A), 935-943.
- Allen, T.I., D.J. Wald, and C.B. Worden (2012). Intensity attenuation for active crustal regions, *J. Seismol.* 16, 409-433.
- Anagnostopoulos S., Providakis S., Salvaneschi P., Athanasopoulou G., Bonaccini G. (2008) SEISMOCARE: An efficient GIS tool for scenario-type investigations of seismic risk of existing cities. *Journal of Soil Dynamics and Earthquake Engineering*, 28:73-78.
- Apostol, B. F. (2010). Elastic waves in a semi-infinite body. *Physics Letters A*, 374, 1601-1607.
- Apostol, B. F. (2017). Elastic waves inside and on the surface of a half-space. *Quarterly Journal of Mechanics and Applied Mathematics*, 70, 3, 289-308.
- Atkinson, G.M. and D.J. Wald (2007). "Did You Feel It?" Intensity Data: A surprisingly good measure of earthquake ground motion, *Seis. Res. Lett.* 78, 362-368.
- Baise, L. G., Kaklamanos, J., Berry, B. M., & Thompson, E. M. (2016). Soil amplification with a strong impedance contrast: Boston, Massachusetts. *Engineering geology*, 202, 1-13.
- Baker, J. W., & Jayaram, N. (2008). Correlation of spectral acceleration values from NGA ground motion models. *Earthquake Spectra*, 24(1), 299-317.
- Balan, S. F., Cioflan, C. O., Apostol, B. F., Tataru, D., Grecu, B. (2008). The resonance of the surface waves. The H/V ratio in the Metropolitan Area of Bucharest. In *AIP Conference Proceedings*, Vol. 1020, No. 1, pp. 207-215.
- Balan, S. F., Tiganescu, A., Apostol, B. F., & Danet, A. (2019). Post-earthquake warning for Vrancea seismic source based on code spectral acceleration exceedance. *Earthquakes and Structures*, 17(4), 365-372. <https://doi.org/10.12989/EAS.2019.17.4.365>
- Boore D.M., Jonathan P. Stewart, Emel Seyhan and Gail Atkinson, (2014) NGA-West2 Equations for Predicting PGA, PGV, and 5 % Damped PGA for Shallow Crustal Earthquakes, *Earthquake Spectra*, 30(3): 1057 - 1085.
- Borcherdt, R.D. (1994). Estimates of site-dependent response spectra for design (methodology and justification), *Earthquake Spectra* 10, 617-654.

- Bratosin D., Apostol B. F., Balan S. F. (2017). Avoidance strategy for soil-structure resonance by considering nonlinear behavior of the site materials. *Romanian Journal of Physics*, 62 (5-6), 808.
- Boulder Real Time Technologies (2007). <http://www.brnt.com> (accessed 12/6/2024)
- Cauzzi C., E. Faccioli, M. Vanini and A. Bianchini (2014) "Updated predictive equations for broadband (0.0 - 10.0 s) horizontal response spectra and peak ground motions, based on a global dataset of digital acceleration records", *Bulletin of Earthquake Engineering*
- Chioccarelli E., Iervolino I. (2024) RINTC Database of fragility functions. Available at <https://www.reluis.it/RINTC-DFF/>. DOI: 10.57580/ReLUIS.WP3DB001
- Chiou, B. S.-J. and Youngs, R. R. (2014), "Updated of the Chiou and Youngs NGA Model for the Average Horizontal Component of Peak Ground Motion and Response Spectra, *Earthquake Spectra*, 30(3), 1117 - 1153, DOI: 10.1193/072813EQS219M
- Cioflan, C. O., Marmureanu, A. and Marmureanu, G. (2009). Nonlinearity in seismic site effects evaluation. *Romanian Journal of Physics*, 54, 951-964.
- Cioflan, C.O., Apostol, B.F., Moldoveanu, C.L., Panza, G.F., Marmureanu, G. (2004). Deterministic approach for the seismic microzonation of Bucharest. *Pure and Applied Geophysics*, 161, 1149–1164.
- Coman, A., Manea, E. F., Cioflan, C. O., & Radulian, M. (2020). Interpreting the fundamental frequency of resonance for Transylvanian Basin. *Romanian Journal of Physics*, 65, 809.
- Convertito, V., & Emolo, A. (2012). Investigating rupture direction for three 2012 moderate earthquakes in northern Italy from inversion of peak ground-motion parameters. *Bulletin of the Seismological Society of America*, 102(6), 2764-2770.
- Convertito, V., Caccavale, M., De Matteis, R., Emolo, A., Wald, D., & Zollo, A. (2012). Fault extent estimation for near-real-time ground-shaking map computation purposes. *Bulletin of the Seismological Society of America*, 102(2), 661-679.
- Cornell, C. A. (1968). Engineering seismic risk analysis. *Bulletin of the seismological society of America*, 58(5), 1583-1606.
- Crowley, H., Pinho, R. & Bommer, J.J. (2004) A Probabilistic Displacement-based Vulnerability Assessment Procedure for Earthquake Loss Estimation. *Bull Earthquake Eng* 2, 173–219. <https://doi.org/10.1007/s10518-004-2290-8>
- Crowley H., Borzi B., Pinho R., Colombi M., Onida M. (2008) Comparison of Two Mechanics-Based Methods for Simplified Structural Analysis in Vulnerability Assessment, *Advances in Civil Engineering*, Article ID 438379
- Crowley H., Despotaki V., Rodrigues D., Silva V., Toma-Danila D., Riga E., Karatzetzou A., Fotopoulou S., Zugic Z., Sousa L., Ozcebe S., Gamba P. (2020) Exposure model for European seismic risk assessment. *Earthquake Spectra* 1-22, doi: 10.1177/8755293020919429
- Crowley H., Dabbeek J., Despotaki V., Rodrigues D., Martins L., Silva V., Romão, X., Pereira N., Weatherill G. and Danciu L. (2021a) European Seismic Risk Model (ESRM20), EFEHR Technical Report 002, V1.0.0, 84 pp, <https://doi.org/10.7414/EUC-EFEHR-TR002-ESRM20>
- Crowley H., Despotaki V., Silva V., Dabbeek J., Romao X., Pereira N., Castru J.M., Daniell J., Veliu E., Bilgin H., Adam C., Deyanova M., Ademovic N., Atalic J., Riga E., Karatzetzou A., Bessason B., Shendova V., Tiganeşcu A., Toma-Danila D., Zugic Z., Akkar S., Hancilar U. (2021b) Model of seismic design lateral force levels for the existing reinforced concrete European building stock, *Bulletin of Earthquake Engineering*, 19:2839–2865, doi: 0.1007/s10518-021-01083-3
- Cultrera, G., Ameri, G., Saraò, A., Cirella, A., & Emolo, A. (2013). Ground-motion simulations within ShakeMap methodology: application to the 2008 Iwate-Miyagi Nairiku (Japan) and 1980 Irpinia (Italy) earthquakes. *Geophysical Journal International*, 193(1), 220-237.
- D'Ayala D. et al. (2021) D4.3 Report on simplified models for the estimation of seismic functional and systemic losses. Responsible Partner: UCL. TURNKEY Project. Available at <https://earthquake-turnkey.eu/deliverables-2/>

- Danciu, L., Giardini, D., Weatherill, G., Basili, R., Nandan, S., Rovida, A., Beauval, C., Bard, P.-Y., Pagani, M., Reyes, C. G., Sesetyan, K., Vilanova, S., Cotton, F., and Wiemer, S. (2024) The 2020 European Seismic Hazard Model: overview and results, *Nat. Hazards Earth Syst. Sci.*, 24, 3049–3073, <https://doi.org/10.5194/nhess-24-3049-2024>
- Danciu L., Nandan S., Reyes C., Basili R., Weatherill G., Beauval C., Rovida A., Vilanova S., Sesetyan K., Bard P.-Y., Cotton F., Wiemer S., Giardini D. (2021) - The 2020 update of the European Seismic Hazard Model: Model Overview. EFEHR Technical Report 001, v1.0.0, <https://doi.org/10.12686/a15>
- Dominguez, R. T., Rodríguez-Lozoya, H. E., Sandoval, M. C., Sanchez, E. S., Meléndez, A. A., Rodríguez-Leyva, H. E., & Campos, R. A. (2017). Site response in a representative region of Manzanillo, Colima, Mexico, and a comparison between spectra from real records and spectra from normative. *Soil Dynamics and Earthquake Engineering*, 93, 113-120. <https://doi.org/10.1016/j.soildyn.2016.11.013>
- Douglas, J., & Gkimprxis, A. (2018). Risk targeting in seismic design codes: the state of the art, outstanding issues and possible paths forward. *Seismic Hazard and Risk Assessment: Updated Overview with Emphasis on Romania*, 211-223.
- Engler, Davis T., C. Bruce Worden, Eric M. Thompson, Kishor S. Jaiswal (2022). Partitioning Ground Motion Uncertainty When Conditioned on Station Data. *Bull. Seism. Soc. Am.* 2022; doi: <https://doi.org/10.1785/0120210177>
- FEMA/NIBS methodology HAZUS®MH MR5 (2003), Advanced engineering building module: technical and user's manual, Federal Emergency Management Agency, Washington DC, USA.
- Field, E. H., Jacob, K. H. (1995). A comparison and test of various site-response estimation techniques, including three that are not reference-site dependent. *Bulletin of the Seismological Society of America*, 85(4), 1127-1143.
- GEM (2024) OpenQuake Manual. Available at <https://docs.openquake.org/oq-engine/latest/manual/>
- Guérin-Marthe, S., Gehl, P., Negulescu, C., Auclair, S., & Fayjaloun, R. (2021). Rapid earthquake response: The state-of-the art and recommendations with a focus on European systems. *International Journal of Disaster Risk Reduction*, 52, 101958.
- Gutenberg, B., & Richter, C. F. (1944). Frequency of earthquakes in California. *Bulletin of the Seismological society of America*, 34(4), 185-188.
- Hardebeck J.L., Llenos A.L., Michael A.J., Page M.T., Schneider M., van der Elst N.J. (2024) Aftershock Forecasting. *Annu. Rev. Earth Planet. Sci.* 2024. 52:61–84. <https://doi.org/10.1146/annurev-earth-040522-102129>
- Hassani, B., & Atkinson, G. M. (2016). Applicability of the site fundamental frequency as a VS 30 proxy for central and eastern North America. *Bulletin of the Seismological Society of America*, 106(2), 653-664.
- Heath, D. C., Wald, D. J., Worden, C. B., Thompson, E. M., & Smoczyk, G. M. (2020). A global hybrid VS 30 map with a topographic slope-based default and regional map insets. *Earthquake Spectra*, 36(3), 1570-1584.
- Helmholtz-Centre Potsdam - GFZ German Research Centre for Geosciences and gempa GmbH. The SeisCompP seismological software package. GFZ Data Services. 2008. URL: <https://www.seiscomp.de>, doi:10.5880/GFZ.2.4.2020.003.
- Julien-Laferrrière S. (2019) Earthquake qualitative impact assessment: Performance evaluation. SERA-JRA6 Report
- Kale O., S. Akkar, A. Ansari and H. Hamzehloo as published in "A ground-motion predictive model for Iran and Turkey for horizontal PGA, PGV and 5%-damped response spectrum: Investigation of possible regional effects", *Bulletin of the Seismological Society of America* (2015), 105(2A): 963 – 980
- Kassaras, I., Papadimitriou, P., Kapetanidis, V., & Voulgaris, N. (2017). Seismic site characterization at the western Cephalonia Island in the aftermath of the 2014 earthquake series. *International Journal of Geo-Engineering*, 8, 1-22.

- Konno, K. and Ohmachi, T. (1998). Ground-motion characteristics estimated from spectral ratio between horizontal and vertical components of microtremor. *Bulletin of the Seismological Society of America*, 88(1):228–241.
- Kramer, S. L. (1996). *Geotechnical Earthquake Engineering*. Prentice–Hall International Series in Civil Engineering and Engineering Mechanics, Prentice-Hall, Upper Saddle River, New Jersey, 653.
- Lermo, J., Chavez-Garcia, F.J. (1993). Site effect evaluation using spectral ratios with only a station. *Bull. Seism.Soc.Am*, 83, 1574–1594.
- Lopez Hidalgo F., M. Navarro and S. Molina, A new tool to simulate ground shaking and earthquake losses, *Rev. int. métodos numér. cálc. diseño ing.* (2022). Vol. 38, (3), 35 URL [https://www.scipedia.com/public/Lopez\\_Hidalgo\\_et\\_al\\_2022b](https://www.scipedia.com/public/Lopez_Hidalgo_et_al_2022b)
- Loth, C., and Baker, J. W. (2013). “A spatial cross-correlation model of ground motion spectral accelerations at multiple periods.” *Earthquake Engineering & Structural Dynamics*, 42, 397–417.
- Malcioglu, F. S., O’Kane, A., Donmez, K., & Aktas, Y. D. (2022). Characteristics of Strong Ground Motions in the 30 October 2020, MW6. 9 Aegean Sea Earthquake. *Frontiers in Built Environment*, 8, 870279. <https://doi.org/10.3389/fbuil.2022.870279>
- Maio R., Tsionis G., 2015. Seismic fragility curves for the European building stock, JRC Technical Report, European Commission
- Manea, E. F., Cioflan, C. O., Coman, A., Michel, C., Poggi, V., & Fäh, D. (2020). Estimating Geophysical Bedrock Depth Using Single Station Analysis and Geophysical Data in the Extra-Carpathian Area of Romania. *Pure and Applied Geophysics*, 1-16.
- Manea, E. F., Coman, A., & Cioflan, C. O. (2021a). Evaluation of the predominant frequency of resonance of sedimentary layers using 2014 5.7 ML Vrancea crustal event records. *Romanian Reports in Physics*, 73(3).
- Manea, E. F., Coman, A., & Cioflan, C. O. (2021b). Evaluation of the predominant frequency of resonance of sedimentary layers using 2014 5.7 ML Vrancea crustal event records. *Romanian Reports in Physics*, 73(3).
- Manea, E. F., Michel, C., Hobiger, M., Fäh, D., Cioflan, C. O. , Radulian, M. (2017). Analysis of the seismic wavefield in the Moesian Platform (Bucharest area) for hazard assessment purposes. *Geophysical Journal International*, 210 (3), 1609-1622.
- Manea, E. F., Michel, C., Poggi, V., Fäh, D., Radulian, M., & Balan, F. S. (2016). Improving the shear wave velocity structure beneath Bucharest (Romania) using ambient vibrations. *Geophysical Supplements to the Monthly Notices of the Royal Astronomical Society*, 207(2), 848-861.
- Manea, E. F., Predoiu, A., Cioflan, C., & Diaconescu, M. (2019). Interpretation of resonance fundamental frequency for Moldavian and Scythian platforms. *Romanian Reports in Physics*, 71, 709.
- Manea, E.F.; Cioflan, C.O.; Danciu, L. (2022) Ground-motion models for Vrancea intermediate-depth earthquakes. *Earthq. Spectra*, 38, 407–431
- Manfredi, V., Nicodemo, G., & Masi, A. (2023). Estimation of Human Casualties Due to Earthquakes: Overview and Application of Literature Models with Emphasis on Occupancy Rate. *Safety*, 9(4), 82. <https://doi.org/10.3390/safety9040082>
- Marmureanu, Gh., Misicu, M., Cioflan, C. O., Balan, S. F., Apostol, B. F. (2005). Nonlinear Seismology – the seismology of the XXI Century, in *Lecture Notes of Earth Sciences*, “Perspective in Modern Seismology”, ed. F. Wenzel, Springer Verlag, Heidelberg, 105, 47-67.
- Marmureanu A., Ionescu C., Grecu B., Toma-Danila D., Tiganescu A., Neagoe C., Toader V., Craifaleanu I.-G., Dragomir C.S., Meita V., Liashchuk O.I., Dimitrova L., Ilie I. (2021) From National to Transnational Seismic Monitoring Products and Services in the Republic of Bulgaria, Republic of Moldova, Romania, and Ukraine. *Seismological Research Letters*, 92 (3): 1685–1703, doi: 10.1785/0220200393
- Martins L., Silva V. (2023), Global Vulnerability Model of the GEM Foundation, GitHub. [https://github.com/gem/global\\_vulnerability\\_model/](https://github.com/gem/global_vulnerability_model/) DOI: 10.5281/zenodo.8391742

- Michel, C., Crowley, H., Hannewald, P., Lestuzzi, P., and Fäh, D. (2018). "Deriving fragility functions from bilinearized capacity curves for earthquake scenario modelling using the conditional spectrum." *Bull. Earthq. Eng.*, 16(10), 4639–4660.
- Molina S., Lang D.H., Lindholm C.D. (2010) SELENA. An open-source tool for seismic risk and loss assessment using a logic tree computation procedure. *Computers & Geosciences*, 36:257-269.
- Moratto, Luca, and Angela Saraò. "Improving ShakeMap performance by integrating real with synthetic data: tests on the 2009 M<sub>w</sub>= 6.3 L'Aquila earthquake (Italy)." *Journal of seismology* 16 (2012): 131-145.
- Nakamura, Y. (1989). A method for dynamic characteristics estimation of subsurface using microtremor on the ground surface. *Rep. Railway Tech. Res. Inst.*, 30(1):25– 33.
- Nogoshi, M. and Igarashi, T. (1971). On the amplitude characteristics of microtremors, Part 2 (In Japanese with English abstract). *J. Seism. Soc. Japan*, 24:26–40.
- Ohmachi, T., Nakamura, Y., & Toshinawa, T. (1991, March). Ground motion characteristics in the San Francisco Bay area detected by microtremor measurements. In *Proc. 2 nd Internat. Conf. on Recent Advances in Geotechniques, Earthquake Engineering and Soil Dynamics*. San Louis, Missouri (pp. 11-15).
- Ordaz, M., Aguilar, A., Arboleda, J. (2007). Program for computing seismic hazard.
- Ozcep, F., Karabulut, S., Korkmaz, B., & Zarif, H. (2010). Seismic microzonation studies in Sisli/Istanbul (Turkey). *Sci. Res. Essay*, 5(13), 1595-1614.
- Papatheodorou K, Theodoulidis N, Klimis N, Zulfikar C, Vintila D, Cardanet V, Kirtas E, Toma-Danila D, Margaris B, Fahjan Y, et al. (2023) Rapid Earthquake Damage Assessment and Education to Improve Earthquake Response Efficiency and Community Resilience. *Sustainability*. 15(24):16603. <https://doi.org/10.3390/su152416603>
- Pitilakis K., H. Crowley, A.M. Kaynia (2004) SYNER-G: Typology Definition and Fragility Functions for Physical Elements at Seismic Risk. Springer Dordrecht. <https://doi.org/10.1007/978-94-007-7872-6>
- Poggi, V., Fäh, D., Burjanek, J., & Giardini, D. (2012). The use of Rayleigh-wave ellipticity for site-specific hazard assessment and microzonation: application to the city of Lucerne, Switzerland. *Geophysical Journal International*, 188(3), 1154-1172.
- Pomonis, A., Kappos, A.J., Karababa, F., Panagopoulos, G., 2009. Seismic vulnerability and collapse probability assessment of buildings in Greece, in: *Second International Workshop on Disaster Casualties*. University of Cambridge, UK.
- Porter, K. (2020) A Beginner's Guide to Fragility, Vulnerability, and Risk. University of Colorado Boulder, <https://www.sparisk.com/pubs/Porter-beginners-guide.pdf>.
- Reiter L. 1991. *Earthquake Hazard Analysis: Issues and Insights*. x+ 254 pp. New York: Colombia University Press.
- Romão X., N. Pereira, J.M. Castro, H. Crowley, V. Silva, L. Martins, & F. De Maio. (2021). European Building Vulnerability Data Repository (v2.1). Zenodo. <https://doi.org/10.5281/zenodo.4062410>
- Rossetto, T., D'Ayala, D., Ioannou, I., Meslem, A., 2014. Evaluation of Existing Fragility Curves, in: Pitilakis, K., Crowley, H., Kaynia, A.M. (Eds.), SYNER-G: Typology Definition and Fragility Functions for Physical Elements at Seismic Risk, *Geotechnical, Geological and Earthquake Engineering*. Springer Netherlands, Dordrecht, pp. 47–93. [https://doi.org/10.1007/978-94-007-7872-6\\_3](https://doi.org/10.1007/978-94-007-7872-6_3)
- Salgado-Gálvez, M. A., Ordaz, M., Huerta, B., Garay, O., Avelar, C., Fagà, E., Kohrang, M., Ceresa, P., Triantafyllou, G., and Begaliev, U. T. (2024) Development of a regionally consistent and fully probabilistic earthquake risk model for Central Asia, *Nat. Hazards Earth Syst. Sci.*, 24, 3851–3868, <https://doi.org/10.5194/nhess-24-3851-2024>
- Seyhan, E. and J.P. Stewart (2014). Semi-Empirical Nonlinear Site Amplification from NGA-West2 Data and Simulations, *Earthquake Spectra* 30(3), 1241-1256.
- Sokolov, V.; Bonjer, K.P.; Wenzel, F.; Grecu, B.; Radulian, M. Ground-motion prediction equations for the intermediate depth Vrancea (Romania) earthquakes. *Bull. Earthq. Eng.* 2008, 6, 367–388

- Su, F., Anderson, J. G., & Zeng, Y. (2006). Characteristics of ground motion response spectra from recent large earthquakes and their comparison with IEEE standard 693. In Proceedings of 100th anniversary earthquake conference, commemorating the (pp. 18-22).
- Theodoulidis, N.; Margaris, B.; Sotiriadis, D.; Zulfikar, C.; Okuyan Akcan, S.; Cioflan, C.O.; Manea, E.F.; Toma-Danila, D. (2024) Rapid Earthquake Damage Assessment System in the Black Sea Basin: Selection/Adoption of Ground Motion Prediction Equations with Emphasis in the Cross-Border Areas. *GeoHazards* 2024, 5, 255-270. <https://doi.org/10.3390/geohazards5010013>
- Thompson, E. M., & Wald, D. J. (2012). Developing VS30 site-condition maps by combining observations with geologic and topographic constraints. In 15th world conference on earthquake engineering, Lisbon, Portugal (Vol. 2428).
- Tiganescu A. et al. (2022) D4.2 Report on recommendations on fragility functions for buildings and infrastructure components to be used in rapid response context. Responsible Partner: EUCENTRE. TURNKEY Project. Available at <https://earthquake-turnkey.eu/deliverables-2/>
- Toma-Danila D., Cioflan C.O. (2021) Îmbunătățirea sistemului pentru estimarea rapidă a pagubelor generate de cutremure în România (SeisDaRo), printr-o mai bună considerare a particularităților hazardului și vulnerabilității locale (chapter 16), In: Cercetări multidisciplinare privind monitorizarea cutremurelor și modelarea fenomenului seismic, ed. Ionescu C., Radulian M., Bala A., Romanian Academy Ed., Bucharest, pp. 389-417, ISBN 978-973-27-3383-7
- Toma-Danila D., Armas I. (2017) Insights into the possible seismic damage of residential buildings in Bucharest, Romania, at neighborhood resolution. *Bulletin of Earthquake Engineering*, 15(3):1161-1184, doi: 10.1007/s10518-016-9997-1
- USGS (2024a) Ground Failure Scientific Background. Available at <https://earthquake.usgs.gov/data/ground-failure/background.php>
- USGS (2024b) Operational Aftershock Forecast. Available at <https://earthquake.usgs.gov/data/oaf/>
- Vacareanu, R.; Radulian, M.; Iancovici, M.; Pavel, F.; Neagu, C. Fore-arc and back-arc ground motion prediction model for Vrancea intermediate depth seismic source. *J. Earthq. Eng.* 2015, 19, 535–562.
- Wald, D. J., Quitoriano, V., Worden, C. B., Hopper, M., & Dewey, J. W. (2011). USGS "Did You Feel It?" internet-based macroseismic intensity maps. *Annals of geophysics*, 54(6).
- Wald, D. J., Worden, C. B., Quitoriano, V., & Pankow, K. L. (2005). "ShakeMap Manual: Technical Manual, User's Guide, and Software Guide." U.S. Geological Survey.
- Worden, C. B., Thompson, E. M., Baker, J. W., Bradley, B. A., Luco, N., & Wald, D. J. (2018). Spatial and spectral interpolation of ground-motion intensity measure observations. *Bulletin of the Seismological Society of America*, 108(2), 866-875.
- Worden, C.B., M.C. Gerstenberger, D.A. Rhoades, D.J. and Wald (2012). Probabilistic relationships between groundmotion parameters and Modified Mercalli intensity in California *Bull. Seism. Soc. Am.* 102(1), 204-221. DOI: 10.1785/0120110156.
- Yepes-Estrada C, Silva V, Rossetto T, et al. The Global Earthquake Model Physical Vulnerability Database. *Earthquake Spectra*. 2016;32(4):2567-2585. doi:10.1193/011816EQS015DP
- You T, Teweldebrhan BT, Wang W, Tesfamariam S. Seismic loss and resilience assessment of tall-coupled cross-laminated timber wall building. *Earthquake Spectra*. 2023;39(2):727-747. doi:10.1177/87552930231152512
- Zhang A., Wang X., Pedrycz W., Yang Q., Wang X., Guo H. (2024) Near real-time spatial prediction of earthquake-triggered landslides based on global inventories from 2008 to 2022. *Soil Dynamics and Earthquake Engineering*, 185: 108890